Mesozooplankton structure and functioning in the western tropical South Pacific along the 20° parallel south during the OUTPACE survey (February –April 2015)

François Carlotti[1], Marc Pagano[1], Loïc Guilloux[1], Katty Donoso[1], Valentina Valdés[2,3], Olivier Grosso[1], Brian P. V. Hunt[1,4,5,6]

[1]Aix Marseille Université, Université de Toulon, CNRS, IRD, OSU PYTHEAS, Mediterranean Institute of Oceanography, MIO, UM 110, 13288, Marseille, Cedex 09, France

[2] Programa de Doctorado en Oceanografía, Departamento de Oceanografía, Facultad de Ciencias Naturales y Oceanográficas, Universidad de Concepción, Concepción, Chile

[3] Laboratoire d'Océanographie Microbienne (LOMIC), Observatoire Océanologique, UPMC Université Pierre et Marie Curie, Univ Paris 06, CNRS, Sorbonne Universités, Banyuls Sur Mer, France

[4]Institute of the Oceans and Fisheries, University of British Columbia, Vancouver, V6T 1 Z4, British Columbia, Canada

[5]Department of Earth, Ocean and Atmospheric Sciences, University of British Columbia, Vancouver, British Columbia, Canada,

[6]Hakai Institute, Heriot Bay, British Columbia, Canada,

Correspondence to: François Carlotti (francois.carlotti@mio.osupytheas.fr)

Abstract.

The western tropical South Pacific (WTSP) is one of the most understudied oceanic regions in terms of the planktonic food web, despite supporting some of the largest tuna fisheries in the world. In this stratified oligotrophic ocean, nitrogen fixation may play an important role in supporting the plankton food web, and higher trophic level production. In the austral summer (Feb-Apr) of 2015, the OUTPACE survey conducted a comprehensive transect of 4000 km along the 20°S south latitude from New Caledonia to Tahiti to determine the role of diazotrophs in this region. Here, we present data on the zooplankton community, with the specific objectives to characterize zooplankton community, and plankton food web processes, including the importance of diazotroph derived nitrogen (DDN) in supporting zooplankton. A total of 15 short-duration stations (8 hours each) were completed to describe the large-scale variation. Three long-duration stations (5 days

each) enabled more detailed analysis of processes, and were positioned: (1) in offshore northern waters of New Caledonia, (2) near Niue Island, and (3) in the subtropical Pacific gyre near the Cook Islands. At all stations, mesozooplankton were sampled with a Bongo Net with 120 μm mesh size and estimates were made of abundance, biomass, community taxonomy and size structure, and size fractionated δ15N. Subsequently, we estimated zooplankton carbon demand, grazing impact, excretion rates, and the contribution of DDN to zooplankton biomass. The mesozooplankton community showed a general decreasing trend in abundance and biomass from West to East, with a clear drop in the ultra-oligotrophic waters of the subtropical Pacific gyre (GY). Higher abundance and biomass corresponded to higher primary production associated with complex mesoscale circulation in the Coral Sea and between the longitudes 170-180°W. The taxonomic structure showed a high degree of similarity in term of species richness and abundance distribution across the whole region, however with a moderate difference in the GY, where the copepod contribution to mesozooplankton increased. The estimates of ingestion and metabolic rates allowed us to estimate that the top-down (grazing) and bottom-up (excretion of N and P) impacts of zooplankton on phytoplankton were potentially high. Daily grazing pressure on phytoplankton stocks was estimated to remove 19 to 184% of the total daily primary production and 1.5 to 22 % of fixed N_2. The top-down impact of mesozooplankton was higher in the eastern part of the transect including GY than in the Coral Sea region and was mainly exerted on nano- and microphytoplankton. Regeneration of nutrients by zooplankton excretion was high suggesting high contribution to regenerated production particularly in terms of nitrogen. Daily NH_4 excretion represented 14.5 to 165 % of phytoplankton needs for N whereas PO_4 excretion accounted for only 2.8 to 34% of P needs. From the quantification of the contribution of DDN to Zooplankton δ15N values, we estimated that DDN contributed up to 67 and 75% to zooplankton biomass in the Western (W-MA) and Central (CE-MA) parts of the Melanesian Archipelago (MA) regions respectively, but strongly decreased to an average of 22% in the GY region and down to 7% in the eastern most station. Thus, highest contribution of diazotrophic microorganisms to zooplankton occurred in the region of highest N_2 fixation and when *Trichodesmium* dominated the diazotrophs. Our estimations of the fluxes associated to zooplankton were highly variables between stations and zones, but very high in most cases compared to literature data, partially due to the high contribution of small forms. The highest values encountered were found at the boundary between the oligotrophic (MA) and ultra-oligotrophic regions (GY). Within the MA zone, the high variability of the top down and bottom-up impacts was related to the high mesoscale activity in the physical environment. Estimated zooplankton respiration rates relative to primary production were among the highest cited values at similar latitudes, inducing a high contribution of migrant zooplankton respiration to carbon flux. Despite the relatively low biomass values of planktonic components in quasi-steady state, the availability of micro- and macronutrients related to physical mesoscale patterns in the waters surrounding the MA, the fueling by DDN, and the relatively high rates of plankton production and metabolism estimated during OUTPACE may explain the productive food chain ending with valuable fisheries in this region.

1 Introduction

The western tropical South Pacific (WTSP) is a vast oceanic area extending from the Coral Sea in the west to the western boundary of the South Pacific Subtropical Gyre (SPSG) in the east, and centered on the 20°S parallel. It is one of the most understudied oceanic regions in terms of the planktonic food web, despite supporting some of the largest tuna fisheries in the world and showing variable production in response to El Niño Southern Oscillation (ENSO) events (Longhurst, 2006; Le Borgne et al, 2011; Smeti et al. 2015; Houssard et al. 2017).

Over the last decade the WTSP has been the subject of a number of studies concerning the biogeographical distributions of picoplankton (see Buitenhuis et al., 2012 for the data synthesis; Campbell et al. 2005) and diazotrophs (Shiozaki et al., 2014; Bonnet et al. 2015, 2017), due to their key roles in biogeochemical cycling and the functioning of oligotrophic subtropical pelagic ecosystems. In this stratified oligotrophic ocean, a major source of new N for the pelagic food web appears to be N_2 fixation by unicellular (Zehr et al., 2001; Campbell et al., 2005; Bonnet et al. 2015) and filamentous cyanobacteria (Bonnet et al., 2009; Moisander et al., 2010; Dupouy et al., 2011). This latter form may accumulate substantial biomass after massive blooms in the summer (Campbell et al., 2005; Dupouy et al., 2011).The contribution of blooms of cyanobacteria to the food web appears to be highly variable, and remains controversial. (Le Borgne et al 2011). Abundances of zooplankton have been linked to blooms of *Trichodesmium* (Landry et al. 2001), but in most cases, a high biomass of cyanobacteria does not result in increase in zooplankton biomass because some cyanobacteria are toxic or unpalatable (Turner 2014). Grazing on *Trichodesmium* has been considered as a food source for only a few zooplankton species, mainly harpacticoid copepods (Hawser et al. 1992; O'Neil and Roman 1994; O'Neil 1998), however, recent studies have provided evidence of zooplankton species feeding on various types of diazotrophs. In the Amazon River plume, copepods were shown to consume diatom-diazotroph assemblage (DDAs) (*Hemialus-Richelia* and *Rhizosolenia-Richelia*, diatom-diazotroph respectively), diazotrophic unicellular cyanobacteria UCYN-A *Candidatus Atelocyanobacterium thalassa*, UCYN-B *Crocosphaera watsonii*, and the colonial cyanobacterium *Trichodesmium* (Conroy et al. 2017). Recently, consumption of UCYN-C by zooplankton was observed in a mesocosm experiment performed in the oligotrophic Noumea lagoon in the southwest Pacific (Hunt et al., 2016), while the *nifH* gene, indicative of N_2 fixation, was measured in the guts of zooplankton including the copepods *Pleuromamma*, *Pontella*, and *Euchaeta* in the western equatorial and subtropical Pacific waters (Azimuddin et al. 2016).

Concomitant surveys planned to identify both diazotroph blooms and zooplankton distributions are rare. The multidisciplinary ANACONDAS program (Amazon River influence on nitrogen fixation and export production in the western tropical North Atlantic) was dedicated to investigating the role of the Amazon plume in stimulating offshore nitrogen fixation, including nitrogen supplied by nitrogen-fixing bacteria, and export production during the river's high-discharge period (May–June 2010). That study showed clear evidence of consumption of DDAs, *Trichodesmium*, and unicellular cyanobacteria by calanoid copepods (Weber et al., 2017; Conroy et al. 2017). In another recent paper, Azimuddin et al. (2016) presented data analysis to understand the diversity and abundance of potentially diazotrophic microorganisms

associated with marine zooplankton, especially copepods. That study was based on the nifH gene in zooplankton samples, mainly copepods, collected in 12 locations in the Pacific Ocean, four stations in the subarctic and subtropical North Pacific, including the ALOHA station, and eight stations in the tropical and subtropical areas of the South Pacific.

5   If we consult the "Copepod database" (https://www.st.nmfs.noaa.gov/copepod/) the Tropical South Pacific Ocean is among the least sampled regions in the word ocean for zooplankton investigation. The most complete ecosystem studies in the region were performed by the US (Murray et al., 1995) and French JGOFS programs (Leborgne & Landry, 2003), in the Equatorial South Pacific (see the review by Le Borgne et al., 2002). These programs included dedicated observations on zooplankton distribution and associated fluxes (White et al., 1995; Zhang et al, 1995; Le Borgne & Rodier, 1997; Le Borgne et al, 1999; Le Borgne et al., 2003). One joint program, Zonal Flux (April l5-May 14, 1996), was an equatorial transect

10   cruise made during a "La Nina" event (April-May 1996) in the equatorial Pacific upwelling. In the WTSP, zooplankton studies are rare and largely confined to the Coral Sea (Le Borgne et al., 2010; Smeti et al 2015). In the eastern tropical South Pacific, regular campaigns of the Scripps Institution of Oceanography in the 1960's provide information on zooplankton taxon distributions (see the review by Fernández-Álamo & Färber-Lorda, 2006).

      The OUTPACE survey (Oligotrophy to UlTra-oligotrophy PACific Experiment, 18 February and 3 April 2015),

15   aboard the RV L'Atalante, was designed specifically to sample a variety of trophic conditions along a west–east transect covering 4000 km in the SE Pacific Ocean from the western part of the Melanesian archipelago (New Caledonia) to the western boundary of the South Pacific gyre (French Polynesia). The aims of the OUTPACE project (Moutin et al. 2017) were (1) to characterize the zonal changes in biogeochemistry and biological diversity across the WSTP during austral summer conditions; (2) to quantify primary production and fate of organic matter (including carbon export) in three

20   contrasting trophic regimes with increasing oligotrophy, with a particular emphasis on the role of dinitrogen fixation in areas of *Trichodesmium* blooms; and (3) to obtain a representation of the main biogeochemical fluxes and dynamics of the planktonic trophic network.

      The primary aims of the present study dedicated to mesozooplankton observations were (1) to document zooplankton density, species diversity, and biomass along the OUTPACE transect, (2) to analyze the relationships between diazotrophic

25   microorganisms and zooplankton, and (3) to characterize the trophic pathways from primary production to mesozooplankton, and in this way to contribute to these three main objectives.

2 Material and methods

2.1 Study site and sampling strategy

      The OUTPACE survey was performed aboard the RV L'Atalante during austral summer conditions between 18

30   February and 3 April 2015 in the WTSP Ocean from New Caledonia (western part of the Melanesian Archipelago) to the French Polynesia, along a West-East transect covering *ca*. 4000km between the latitudes 17°S and 22°S (**Fig. 1**). This region

is impacted by ENSO, known to be the most important mode of SST variability on interannual to decadal timescales (Sarmiento and Gruber, 2006). The year 2015 was classified as an El Niño event, which was reflected on SST and chl-*a* satellite data (Moutin et al., 2017). Along this transect, two types of stations were sampled (**Fig. 1**): 15 short-duration stations (SD1 to SD15, 8 h) dedicated to a large-scale description, and three long-duration stations for Lagrangian process studies, respectively LD A station (19°12.8'S - 164°41.3'E, 25 Feb.-2 Mar.) positioned in western Melanesian archipelago waters in the western part of the transect offshore New Caledonia, LD B station (18°14.4'S - 170°51.5'W, 15-20 Mar.) in the eastern part of Melanesian archipelago waters near Niue Island, and LD C station (18°25.2'S - 165°56.4'W, 23-28 Mar.) in the eastern part of the transect, in the subtropical Pacific gyre near the Cook Islands. All general characteristics of the stations are presented in Moutin et al. (2017, their Table 1).

Real-time-satellite images (altimetry, SST, ocean color) combined with drifter trajectories initiated during the first part of the cruise were used to define the best positions of these three stations using two criteria: sea surface chlorophyll levels to characterize the main sampled regions and minimal current intensity in each region to increase the chance of sampling an homogeneous water mass (Moutin et al, 2017; De Verneil et al., 2018). LD-A and LD-B stations were characterized by local maxima of sea surface chl-*a* to sample the Melanesian Archipelago zone whereas chl-*a* minima characterized LD-C representing typical waters of the subtropical gyre.

2.2 Mesozooplankton sampling

Zooplankton collection was conducted at 14 of the SD stations (the station SD-13 was not sampled for zooplankton) and at the 3 LD stations. SD stations were generally sampled during the day except for SD-04 and SD-05 whereas LD stations were sampled once during the day and once during the night for each of the 5 days of station occupation. Sampling was done with a Bongo Net (70 cm mouth diameter) with 120 μm mesh nets mounted with filtering cod-ends. The nets were equipped with Hydrobios flowmeters. Hauls were done from 200m depth to the surface at a speed of 1 m.s^{-1}. One of the cod-ends was used for biomass measurements. The second one was preserved in 4% buffered formaldehyde for later taxonomic identification, abundance and size spectrum analyses. Volume filtered by the nets (V) was calculated using the formula: V= R* S * K, combining the flowmeter counts, (R, one count is a tenth of revolution), the mouth area of the net (S=0.38 m^2), and the pitch of the impeller of the flowmeter (K) provided by the manufacturer, and equals to 0.03 m count^{-1}.

2.3 Dry weight measurement

The biomass sample was processed onboard. Just after collection, each sample was filtered onto a pre-weighed GF/F filter (47 mm) and oven dried at 60 °C for 2 days. The average biomass concentration (in mg DW m^{-3}) in the upper 200 m was calculated from the zooplankton dry weight (mg), obtained as difference between the weight of the filter with and

without the sample taking in account the water column sampled volume. Biomass was also expressed in carbon, using a C/DW ratio equal to 0.45.

2.4. Identification, abundance and individual size and weight of the zooplankton taxa

5   The taxonomic composition was determined for each formalin sample. Samples were split using a Motoda box, and at least 100 individuals of the more abundant taxa were counted in each sub-sample under a dissecting microscope, a LEICA MZ6. Species/genus identification was made according to Rose (1933), Tregouboff and Rose (1957) and Razouls et al. (2005-2017). The abundance of the various taxa (groups, genera or species) was divided by the sample volume to get concentration of individuals per cubic meter (ind.m^{-3}). The diversity of the zooplankton was determined using the Shannon-

10   Weaver index (Shannon and Weaver, 1949).

Approximates of the individual size (total length) and relative dimensions (length/width) of the different taxa were computed from literature values: summarized data for copepod species in Razouls et al. (2005-2017), mean size values of the other taxa from Tregouboff and Rose (1957) and Conway et al (2003).

For comparison with Zooscan results (see below), we computed the area of each taxa (A) from its dimensions to

15   calculate its equivalent circular diameter (ECD):

$$ECD = \sqrt{\left(4 * \frac{A}{\pi}\right)}$$

We also estimated individual dry weight (DW) using the area-dry weight relationships obtained by Lehette and Hernández-León (2009) for subtropical copepods and mesozooplankton.

2.5 Abundance, biomass and size structure using the Zooscan

20   Samples were digitized with the ZooScan digital imaging system (Gorsky et al., 2010) to determine the size structure of the zooplankton communities, as detailed in Donosoet al (2017). Each sample was divided into 2 fractions (<1000 and > 1000µm) and each fraction was then split using a Motoda box until it contained approximately 1000 objects. The resulting samples were poured onto the scanning cell and zooplankton organisms were manually separated with a wooden spine in order to avoid overlapping organisms. After scanning, each image was processed using ZooProcess using the image analysis

25   software Image-J (Grosjean et al., 2004; Gorsky et al., 2010). Only objects having an equivalent circular diameter (ECD) of > 300µm were detected and processed. Finally, Plankton Identifier software (http://www.obs-vlfr.fr/~gaspari/Plankton_Identifier/index.php) was used for automatic classification of zooplankton into 12 categories. Among them two categories of non-zooplankton organisms, aggregates and fibers were grouped as detritus. A training set of about 1000 objects selected automatically from different scans was used to discriminate and classify between organisms,

30   aggregates and fibers. Afterwards, each scan was corrected using the automatic analysis of images.

Zooplankton abundance estimated from Zooscan (ind m^{-3}) was calculated from the number of validated vignettes in Zooscan samples, taking into account the scanned fraction and the sampled volume from the net tows. Zooplankton estimated dry weight of each vignette was calculated from its area using the regression equation obtained for mesozooplankton by Lehette and Hernández-León (2009).

Below, the terms "ZOOSCAN abundance" and "ZOOSCAN biomass" will indicate values derived from the laboratory ZOOSCAN processing. The abundance and biomass of organisms were first calculated for four size fractions (< 500, 500–1000, 1000–2000 and > 2000 μm) based on their ECD, and then summed to deliver the total average abundance and biomass per sample over the upper 200 m.

2.6 Stable isotope analysis

Nitrogen isotope ratios (δ^{15}N) were measured for the zooplankton size fractions collected for biomass measurement and for particulate organic matter (POM) samples collected at 5 m depth at each station. Zooplankton samples were first homogenized using a mortar and pestle, and packaged into ~ 1 mg sub-samples. For POM analyses, water samples were collected in 4.4L polycarbonate bottles at depth corresponding to 50% and 1% of light attenuation. The samples were immediately filtered on pre-burnt (450 ° C, 4 h) 25 mm GFF filters. Stable isotope analysis was performed with an Integra CN, SerCon Ltd. EA-IRMS. δ^{15}N values were determined in parts per thousand (‰) relative to the external standard of atmospheric N. Repeated measurements of an internal standard indicated measurement precision of ± 0.13 ‰ for δ^{15}N.

The mean δ^{15}N value for each station was calculated as the mean of all size fractions, weighted by size fraction biomass. Subsequently, the contribution of DDN (%) to zooplankton δ^{15}N (ZDDN) values at each station was calculated using a two source mixing model following (Sommer et al., 2006):

$$\% \text{ ZDDN} = 100 * \left(\frac{\delta15N_{zpl} - \delta15N_{zplref}}{TEF + \delta15N_{diazo} - \delta15N_{zplref}} \right)$$

where δ^{15}N$_{zpl}$ is the isotopic signature of the zooplankton collected; TEF is the trophic enrichment factor; δ^{15}N$_{diazo}$ is the isotopic signature of diazotrophs; δ^{15}N$_{zplref}$ is the isotopic signature of zooplankton assuming nitrate based phytoplankton production. TEF and δ^{15}N$_{diazo}$ were set respectively at 2.2 ± 0.3 ‰ (McCutchan et al., 2003; Vanderklift and Ponsard, 2003) and in a range of -1 to -2 ‰ (Montoya et al., 2002). δ^{15}N$_{zplref}$ was set at 6 ‰ for the Melanesian Archipelago stations - a value calculated for the ocean west of New Caledonia where nitrogen fixation is reduced (Hunt et al., 2015) – and at 10.73 ‰ for the GY samples- the mean value of POM samples in the GY+ 2.2 ‰ trophic enrichment for the primary consumer level-. Minimum, average and maximum % ZDDN were estimated using the lower, mean and upper bounds of TEF and the δ^{15}N$_{diazo}$ values cited above.

2.7 Other data from OUTPACE survey used for interpretation and comparison

Acquisition of environmental data used in the present paper is presented in different companion papers. Briefly,temperature, salinity, and density were collected with a CTD SeaBirdSBE 9 and particle distribution with a underwater vessel profiler (UVP), both mounted on a rosette (de Verneil et al, 2018), whereas chlorophyll-a and pheophytin concentrations were estimated for different depths from bottle water samples using the fluorometric method (Dupouy et al, 2018). The depth of the mixed layer (MLD) was calculated using a threshold density deviation of 0.03 kg m^{-3} from the value at a reference depth (de Verneil et al, 2018).

Integrated Chl-*a* and POC were calculated from water samples collected at standard depths from the surface to 200 m using Niskin bottles (see Spungin et al. 2018 for methodological details). Phytoplankton carbon biomass was estimated from Chl-a using a C/Chl-a ratio of 50:1. Abundance and distribution of unicellular (UCYN-A1, UCYN-A2, UCYN-B and UCYN-C), and filamentous heterocystous (het-1) and non-heterocystous (*Trichodesmium*) diazotrophic microorganisms for all stations were taken from Stenegren et al. (2018, their Figure 2). Primary productivity was determined using a ^{14}C labelling method according to Van Wambeke et al (2018).

A drifting array equipped with three PPS5 sediment traps and various captors was deployed at each LD station for 5 days at 3 depths (see Caffin et al., 2018a). Swimmers found in the trap were quantified and genera identified, and weighted. Zooplankton C (Zoo-C), N (Zoo-N) and P (Zoo-P) mass measured at each depth of each station (see methods in Caffin et al., 2018a). Only data from the sediment trap situated at 150 m deep were used here.

2.8. Estimation of zooplankton carbon demand and grazing impact and of zooplankton excretion and respiration rates

The zooplankton carbon demand (ZCD in mgC m^{-3} d^{-1}) was computed based on estimates of biomass and of ration for each taxa:

$$ZCD = Ration \, B_{zoo}$$

where B_{zoo} is the biomass of zooplankton in mgC m^{-3}, and $Ration$(d^{-1}) is the amount of food consumed per unit of biomass per day, calculated as:

$$Ration = (g_z + r) / A \quad \text{with} \quad r = r_b + r_a$$

where g_z is the growth rate of zooplankton, r is the weight specific respiration, with basal (r_b) and active (r_a) components, and A is assimilation efficiency.

Following Nival et al. (1975), we considered a constant values of $A = 0.7$ d^{-1}. For respiration, we applied a constant value for basal respiration (r_b=0.20 d^{-1}) derived from Hernández-León et al. (2008) for 20°S zooplankton and assumed a activity-dependent respiration proportional to growth rate (r_a=0.25 g_z) following Kiørboe et al. (1985).

g_z was calculated following Zhou et al.(2010):

$$g_z(w, T, C_a) = 0.033 \left(\frac{C_a}{C_a + 205 e^{-0.125T}} \right) e^{0.09T} w^{-0.06}$$

as a function of sea water temperature (T, °C), food availability (C_a, mgC m^{-3}, estimated from Chl-a), and weight of zooplankton individuals (w, mgC). C_a was used for herbivorous and omnivorous zooplankton taxa, and replaced by POC for carnivorous zooplankton.

ZCD were thus estimated for each taxa and then summed to estimate ZCD of total zooplankton. We considered two components, one for herbivorous and omnivorous zooplankton (ZCD$_H$), and one for carnivorous zooplankton (ZCD$_C$).To estimate the potential clearance of phytoplankton by zooplankton, we compared ZCD$_H$ to the phytoplankton stock, converted to carbon assuming a classical C:Chl-a ratio of 50:1, and to the phytoplankton primary production estimated by Van Wambeke et al (2018). To estimate the grazing impact on phytoplankton size-classes (pico-, nano- and micro-phytoplankton), we applied the empirical relationship given by Wirtz (2012) to estimate the optimal prey size (D$_{opt}$, as µm equivalent spherical diameter) from the predator size (DZ, as µm ESD):

logD$_{opt}$ = -1.3 + 0.75 log DZ.

According to the root mean square deviations in log(D_{opt}) of the Wirtz's regression model, we assumed a ±60% food-size range around D$_{opt}$ for each zooplankton taxa. When the calculated size range straddles the separation value between two phytoplankton size-classes (e.g., 2µm between pico- and nanoplankton), we assume that the grazing pressure on each phytoplanktonic class is proportional to the distance between the limit of the range and this separation value. Therefore, for each grazer, we implicitly assumed a constant clearance over the prey particle-size range.

Ammonium and phosphorus excretion rates were estimated for each taxa and station from the multivariate regression equations by Ikeda (1985) in which independent variables are animal body weight (carbon) and temperature. The daily NH$_4$ and PO$_4$ excretion values by total zooplankton equal the sum of values for all taxa. To estimate the potential contribution of zooplankton excretion to N and P requirements for phytoplankton, we estimated the latter from primary production using Redfield's ratios.

The contribution of migrating zooplankton to carbon export by respiration and excretion in deep water during the day was estimated at the long duration stations by applying the respiration and excretion rates over twelve hours to the biomass migrating in depth (difference of integrated 0-200m zooplankton net biomass between night and day).

2.9 Data analysis

Principal component analysis (PCA) was used to explore spatial patterns of the environmental variables data characterizing the zooplankton habitat: temperature, salinity, chlorophyll-a, percentage of chlorophyll a (ratio Chl-a/Chl-a+Phae) (average values between 0-200m depth, to be consistent with the net haul depth), depth of the mixed layer (MLD). The data were normalized before the analyses run using the Primer 6.0 software.

One-way or two-way analyses of variance were run, to explore the differences between day and night samples and between stations or zones for the environmental and zooplankton parameters. Post-hoc Scheffe´ tests were performed to

analyze paired differences. Spearman's rank-correlations (Rs) were computed to test relationships between zooplankton variables and environmental parameters. Diversity was calculated for zooplankton and copepod taxa using the Shannon–Wiener diversity index.

Spatial variations of the zooplankton community composition were investigated using multivariate analysis, specifically Nonmetric Multidimensional Scaling (NMDS). A matrix species − stations of square root transformed abundance data was used to estimate station similarity using the Bray Curtis metric. The similarity matrix was then ordinated using NMDS. A SIMPER (percentage of similarity) analysis was performed to identify the species contributing most to similarity or dissimilarity between stations for the station groups identified by NMDS.

Finally, to select the environmental variables "best explaining" community patterns, we used the BEST procedure with the BIOENV algorithm which maximizes a rank correlation between the environmental and zooplankton resemblance matrices. The used environmental variables are the same as used in the PCA and we also considered the abundance of *Trichodesmium*, derived from Stenegren et al. (2018). Analyses were run using Primer 6 for PCA and NDMS and with Statistica v.6 for ANOVA, regression and correlation.

3 Results

3.1 Hydrology and trophic conditions along the transect

In the PCA of environmental data, the first two axes explained 70% of the total variance of which 50% was accounted for by the first axis (**Fig 2**). The first axis clearly separated the Subtropical Gyre (GY) stations (stations LD-C, SD-14 and SD-15), characterized by low chlorophyll but high temperature, salinity and MLD values, from the stations of the Melanesian Archipelago (MA). The second axis opposed two clouds of stations within this latter group: the first included the western stations close to Noumea and the Loyalties (W-MA) and LD-B sampled in "blooming" condition (called BL) and characterized by higher percentage of chlorophyll *a* to total pigments (>67%); and the second cloud (57±0.09% Chl-*a*) grouped the stations referred to as central and eastern MA stations (CE-MA). Mean values of environmental data in each cloud are given in **Table 1**. Salinity was significantly lower in NA than in GY and BL (ANOVA; p<0.05), temperature was significantly lower in MA than in GY, and MLD was significantly deeper in GY than in W-MA and CE-MA (p<0.05). Chl-*a* was significantly lower in GY than in the three other zones and % Chl-*a* was significantly higher in W-MA and BL than in GY and CE-MA.

3.2 Spatial variations of zooplankton, abundance biomass and size structure

The total zooplankton abundance estimated from microscope counting (**Fig. 3A**) and the total zooplankton biomass estimated from cumulated biovolumes of organisms counted with microscope (total or fraction <300 μm) and Zooscan (fraction >300 μm) (**Fig. 3B**) showed a general decreasing trend from West (SD-1) to East (SD-15), with local increases

sometimes linked with Chl-*a* increase (**Tables 2 and 3**). Detritus biomass (estimated with Zooscan) were also particularly high (40-50%) in the Coral Sea region (SD-1 to SD-5 and LD-A), compared to other regions (17% to 44%) (**Fig. 3B and Table 3**). With the exception of stations SD-2, SD-3, and SD-9, total dry weights estimated from the biovolumes of counted organisms and particles (from binocular for ECD <300 µm, and from ZOOSCAN for ECD > 300 µm) showed a good correspondence to measured total dry weight (Rs=0.721, p=0.001). In addition, total dry weights estimated from the ZOOSCAN were well correlated with those estimated from binocular counting for the same size fraction (ECD >300 µm): Rs=0.657, p=0.02. The total zooplankton abundance varied from 409 to 2017 ind m^{-3} (**Fig. 3A and Table 2**). Highest values, but high variability as well, was observed in the New Caledonia region (SD1 to 4, and LD-A). There was a clear drop in abundance in GY stations (LD-C, SD-14 and SD-15) compared to all the other zones (W-MA, CE-MA and BL; p<0.05). Microscope abundance showed relatively good agreement with ZOOSCAN abundance for the size-fraction > 300µm ECD (Rs=0.627, p=0.007). This fraction represented 49 to 63% of the total microscope counted zooplankton abundance (**Fig 3A and Table 2**) whereas it represented 88 to 98% in terms of zooplankton biomass, and was equally distributed in the different size classes, although with stronger variations for the >200 µm size-class. The ratio of abundance of zooplankton size fractions above and below 300µm ECD did not show any spatial trend.

Zooplankton abundance was negatively correlated with water column temperature (Rs=-0.511, p= 0.028) and MLD (Rs=-0.790, p=0.000). It was positively correlated with Chl-*a* (Rs=0.498, p=0.042) when considering all of the transect stations, but the correlation was negative for stations in the New Caledonia region (SD1 to 4, and LD-A; Rs=-0.900; p=0.037) and highly positive for other stations (SD-5 to SD-15, LD-B and LD-C; Rs=0.804; p=0.002). Dry weight (weighed) as well as Zooscan zooplankton biomass (**Fig. 3B and Tables 1 and 3**) were both positively correlated with Chl-*a* (R$_S$=0.588, p=0.013 and Rs=0.68, p=0.002 respectively). As for abundance, better correlations were found when considering stations SD-5 to SD-15 and LD-C, (RS=0.783, p=0.002 for both variables), whereas negative correlation was found with Zooscan zooplankton biomass for stations of the Coral Sea (Rs=-0.900, p=0.035). Interestingly, detritus biomass was also well correlated with Chl-*a* when considering the whole transect data (Rs=0.721, p=0.001) and data from stations outside the Coral Sea (Rs=0.755, p=0.004).

3.3 Taxonomic diversity in the different oceanic regions along the transect

From the 120 µm mesh size Bongo net, 66 zooplankton taxa were identified (**See Supplementary Table 1**) with 41 genera/species of copepods plus miscellaneous nauplii and copepodites). The total number of zooplankton taxa per sample varied from 25 to 40 and the Shannon index between 3.3 and 3.76 bit ind^{-1} (**Table 4**). These two variables displayed their minimal mean values in the GY zone. Copepods were the most abundant group (68 to 86% of total abundance) with a slight increase of their contribution from west to east (see **Table 2**) with a corresponding decrease of other contributors (gelatinous plankton and other holoplankton). Thus, copepod dominance was more prominent in the GY zone (79 to 86%) than in the other sites (<80%). Among copepods, early life stages were dominant (69-88% of copepod abundance) and included mostly copepodites (42-82%). In the GY zone the proportion of adults (mean=15 ± 2%) was lower than in the 3 other zones

(mean>18%), whereas the percentage of adult females was the lowest in W-MA. *Clausocalanus/Paracalanus* (25% of copepod abundance), *Oithona* (19%), *Oncaea* (18%), *Corycaeus* (7.6%) and *Microsetella* (4.6%) were the most abundant copepod genera and were present in all stations sampled. All of these copepod taxa were listed in the top ten species with respect to frequency of abundance for the 4 regions (**Table 5**) along with appendicularians, thecosomata, chaetognaths (except GY). Gelatinous zooplankton represented 8.3 to 24.3% of zooplankton abundance (see **Table 2**) with lowest contributions in stations LD-C and SD-15 in the GY zone. They were dominated by appendicularians (8-17%) and chaetognaths (0.8-3.3%) whereas siphonophores, doliolids, salps and hydrozoans represented <0.5% of the total zooplankton abundance. Chaetognaths were rare in the GY zone (<1%) and at SD-1 (0.2%). Other holoplanktonic taxa (2.3-12.7%) included Thecosomata (1.2-10.2%), Ostracods (1-4%) and Euphausiids (<1%). Meroplankton were mostly polychaete larvae (0.2-0.5%) and lamellibranch larvae (0.1-0.4%), present in the 4 zones.

The NDMS ordinations based on the relative abundance of the zooplankton taxa discriminated GY stations from the other stations (**Fig 4A**, dissimilarity = 20%) mainly due to the contributions of *Corycaeus* (7%) and *Clausocalanus/Paracalanus* (6.3%) which were positively correlated to GY, and Appendicularians (5.6%) and Chaetognaths (5%) which were correlated to the other stations (**Fig. 4B**). However, the analysis did not discriminate groups among W-MA, BL and CE-MA stations, despite these groups being distinguishable on the basis of environmental data.

3.4 Relationships between zooplankton taxa and diazotrophic microorganisms

According to the BEST procedure, the environmental variables best explaining the zooplankton community pattern were *Trichodesmium* abundance, MLD, and Chl-*a* (r=0.593, p=0.05), whereas temperature, salinity and unicellular (UCYN) or heterocystous (het-1) cyanobacteria were not selected. The abundance of major zooplankton taxa along the transect showed a strong positive link with the abundance of diazotrophic microorganisms (**Fig.5**). Positive correlations were found between heterocysted cyanobacteria HET-1 and *Microsetella* (Rs=0.52; p=0.032, *Clauso/Paracalanus* (Rs=0.61; p=0.009), *Oithona* (Rs=0.66; p=0.004) and Appendicularia (Rs=0.53; p=0.030), and between UCYN B and Ostracoda (Rs=0.61; p=0.009). Only *Macrosetella gracilis* (Rs=0.684, p=0.002) and *Oncaea* (Rs=0.484, p=0.049) showed a significant relationships with *Trichodesmium*. Among non-copepod taxa, only Thecosomata, showed a positive correlation with *Trichodesmium* (Rs=0.631, p= 0.007) and displayed significant lower abundance in GY compared to W-MA, CE-MA and BL.

3.5. Temporal dynamics of zooplankton at the three long duration stations and comparison with sediment trap content.

In LD-A and LD-B, the zooplankton biomass observed each day (**Fig. 6A**) showed a dome-shaped pattern with an increase over the 3 first days followed by a decrease. In both stations, successive day-night samples showed a biomass increase during the night, mainly due to the size fraction > 2000 µm (euphausids, large copepods, etc.). In station LD-C, the zooplankton biomass was rather stable over the 6 days without day-night variations. In LD-A and LD-B the proportion of

detritus found in the sample was high, and appeared to increase in LD-A. In LD-A, we observed a much higher abundance at day 5 that at day 1, which did not follow the biomass pattern, whereas in LD-B and LD-C the abundance was rather stable (**Fig. 6B**). Interestingly, the taxonomic distribution in the 3 stations (**Fig. 7A**) showed a stable structure for LD-B and LD-C, but a relative increase of small forms (nauplii, small copepods) parallel to a Chl-*a* increase for LD-A. In LD-B, abundance and biomass of zooplankton did not respond to the crash of the bloom within the last two days. In LD-C the stability of both abundance and biomass was parallel to the stability of Chl-*a*.

In the sediment traps situated at 150 m, there was a more important relative contribution of copepods in LD-C compared to LD-A and LD-B, as observed in the water column (**Fig 7B**). Conversely, appendicularians were a large contributor of the swimmers found in the LD-C trap compared to their frequency in the water column, and by comparison to their respective frequencies in LD-A and LD-B. In LD-B, there was a sharp decrease of swimmers over time in the traps mainly due to copepods, but a relative increase of Ostracods. Pteropods had high relative contribution in the traps (20-30% in LD-A, around 10% in LD-B and LD-C), whereas their relative abundance in the water column was low (1-4%).

3.6 Estimation of fluxes related to mesozooplankton

Biomass weighted zooplankton $\delta^{15}N$ values were lower in the regions W-MA and CE-MA, averaging 2.7‰ and 2‰ respectively, than in the GY were zooplankton $\delta^{15}N$ values averaged 8.5‰ (**Figure 8A**). The $\delta^{15}N$ values of the zooplankton corresponded with those of the POM, being lower west of the GY and increasing in the GY. We estimated that DDN contributed an average of 67 and 75% to zooplankton biomass in the W-MA and CE-MA regions respectively (**Figure 8B**). In the GY, the diazotroph contribution to zooplankton biomass decreased to an average of 22%, and showed a declining trend from west to east with the lowest value of 7% occurring at SD-15. The integrated phytoplankton standing stock derived from water column integrated content of total chlorophyll a within the euphotic layer (**Table 6**) was highest at the LD-B and the lowest in the GY, although the stock generally decreased from West to East along the transect, as seen in Fig 3A with the Chl-*a* distribution pattern. Interestingly, regions with the lowest phytoplankton stocks (GY and CE-MA) presented the highest POC/phytoplankton biomass ratio, 3.73 and 3.67 respectively, whereas this ratio decreased to 2.46 in BL and to 2.60 in W-MA. The average zooplankton weight specific rates of ingestion, NH_4 and PO_4 excretion, and respiration (**Table 6**) determined from allometric relationships for all zooplankton taxa (see Material and Methods) were found to be rather stable over the different regions - although the test identified different ingestion in W-MA and GY-, which reflected narrow variations in temperature, and optimal available food supply (considering the contribution of phytoplankton and POC for the whole zooplankton community). The ingestion by herbivorous/omnivorous zooplankton (ZCD_H) represented between 19 % and 183% of the estimated primary production over all stations, but this percentage was very heterogeneous in CE-MA (with an average of 72.6%), more stable in other region and fell to 34.8 % in W-MA including LD-A. The grazing impact on the phytoplankton stock increased from east to west, but was less in GY (9.4%) than BL (17.6%). Impact on picoplankton was low (<0.25% stock d^{-1}) in all locations, and the grazing was distributed between nano- and microplankton in comparable

proportion, with values particularly high in BL (mean = 73.45and101.54% of the stock per day, for nano and microplankton respectively).

Weight specific excretion rates varied between 0.11 and 0.14d^{-1} for NH$_4$ and between 0.09 and 0.11d^{-1} for PO$_4$. Daily regeneration by zooplankton represented between 29.7 and 77.2% of phytoplankton needs for N and between 5.9 and 165.6% for P. Lowest and highest impacts of zooplankton on phytoplankton in terms of grazing and regeneration were found in the W-MA and CE-MA respectively. Depth integrated zooplankton respiration varied between 50.6 and 248.8 mgC m^{-2} d^{-1} and was significantly lower in GY than in W-MA, CE-MA and BL (**Table 6).** The percentage of estimated zooplankton respiration rates to primary production were the lowest in the W-MA region (7 to 25%), compared to the rates in CE-MA (12 to 112%), BL (30%), GY regions (26 to 52%).

Biomass of migratory zooplankton to deep water during the 12 hour daylight period was estimated from the difference of night and day biomass at the 3 long duration station along with associated fluxes. The strongest impact of diel migration was observed in LD-A where half of the zooplankton biomass migrated, injecting 20% of the surface zooplankton carbon biomass through respiration below 200 m. Biomass of migratory zooplankton and respiration below 200 m were reduced to a half in LD-B, whereas no migration could be estimated in LD-C from our net tows. However, in term of percentage of the primary production, the carbon released by zooplankton respiration below 200 m was comparable in the two stations LD-A and LD-B (3 and 3.75 %, respectively). The daily biomass of zooplankton trapped in the sediment traps situated at 150 m at the LD stations were around 50 mgCm^{-2} d^{-1} with no significant difference between stations (**Table 6**). In LD-A and LD-B, it represented respectively 12.7 and 30.1 % of the migrating biomass.

4 Discussion

4.1 What the OUTPACE transect contributes to the characterization of Longhurst (2006)'s provinces ARCH and SPSG

The OUTPACE campaign delivered a unique 4000 km zonal transect across the South Western Tropical Pacific straddling the 20°S latitude. This transect spanned two regions previously defined by Longhurst (2006): the south eastern part of the Archipelago Deep Basins Province (ARCH), a province of diverse basins of the Indo Pacific archipelago amongwhich the Coral Sea visited during OUTPACE is the largest one; and the north western part of the South Pacific Subtropical Gyre Province (SPSG). Along the 20°S parallel, the transition between the two regions during OUTPACE was estimated to be west of Niué Island, (19°05 S, 169°52 W)between the LD-B and LD-C stations (Moutin et al. 2017). The LD-C station was performed in a cyclonic eddy in the most oligotrophic part of the OUTPACE transect close to the Cook Islands and our PCA grouped it in a cloud of stations includingSD-14 and SD-15 (GY) which clearly belong to the SPSG region. The position of LD-B relative to the region ARCH or SPSG is more debatable. LD-B was situated east of the Tonga trench, whereas SD-12 was just north of the trench and SD-11 west of Tonga Island with a bottom depth of 2500m. The PCA

situated the LD-B station between LD-C (GY group) and SD-12 (CE-MA group) on the first axis (see **Fig. 2**), however due to the high Chl-*a* values, LD-B was excluded from GY and CE-MA. The LD-B position was chosen on board, the survey strategy being modified by the development of tropical cyclone Pam, and was further east than initially planned. Therefore, it is possible that at this latitude (20° S), the position of the limit between ARCH and SPSG is west of LD-B, at the level of Tonga Trench, and that LD-B presented special conditions due to the storm in the most western part of SPSG.

As mentioned by Longhurst (2006), the ARCH province is a mosaic of different regions. During OUTPACE, two sub-regions were differentiated by PCA (**Fig. 2**). The first, W-MA in the North of New Caledonia (SD-1 to 3 and LD-A – MAW in Moutin et al., 2018)and the second, CE-MA, through the tropical islands east of New Caledonia (eastern part of the Coral Sea), south of Vanuatu and Fiji islands, and north as far as Tonga islands (SD-4 to SD-12 - MAE in Moutin et al., 2018). The limit between the two regions in the Coral Sea is linked to the seasonal position of the South Fiji jet and the bathymetry (Ceccarelli et al 2013). During OUTPACE, SD-4 and SD-5, at the northern frontier of the Norfolk ridge and upon the New Hebrides trench, under the influence of the South Fiji jet, were grouped with the CE-MA station in our PCA.

4. 2. Spatial structure of zooplankton biomass and abundance related to physical and biogeochemical environment

The distribution of mesozooplankton abundances and biomasses during OUTPACE presented a decreasing West-East gradient. The pattern followed the sea surface chlorophyll gradient, which in turn reflected the oligotrophic gradient with higher values obtained at W-MA, intermediate values at CE-MA, and lowest values at GY (Moutin et al., 2017). We found a positive correlation between zooplankton biomass (and abundance) and Chl-*a* from stationsSD-5 to SD-11, but a negative correlation in the Coral Sea stations SD-1 to SD-4. During OUTPACE the highest zooplankton biomass was found in the CE-MA region (LD-A, SD4 and SD5), but high values were also found at LD-B, and to a lesser extent at SD-9. In all cases, these higher values were associated with productivity enrichment linked to mesoscale features (Rousselet et al. 2018, their Fig; 3, top panel). The survey path from stations SD1 to SD5 passed through a succession of cyclonic and anti-cyclonic eddies, but the distance between sampling stations was unfortunately not well enough resolved to map them. A few studies have related the impact of mesoscale structure on zooplankton distribution in the region (Le Borgne et al. 1985; Smeti et al, 2015). Around Mare (the southernmost Loyauté Island), Le Borgne et al. (1985) found similar zooplankton enrichment, not correlated with chlorophyll increase but associated with diverse mesoscale processes and in particular the island mass effect leeward (west) of Mare. It can be expected that such patterns are general features in regions where zooplankton aggregations occur more in flow-disturbed areas than in free stream jets (Rissik et al., 1997). In such regions, nutrient injections into the euphotic layer may cause intermittent short-lived phytoplankton production enhancement. However, zooplankton biomass increase may lag the phytoplankton production increase by a couple of weeks, a duration equivalent of the average development time of zooplanktonic organisms at local temperatures. In the long duration stations LD-A and LD-B, chosen to understand the impact of ephemeral blooms on the ecosystem response and fate of the primary production, the zooplankton population responded with a large production of larval forms over the 5 days station occupation, but this response yielded

limited biomass changes. Other mesoscale activities were observed in the CE-MA region during OUTPACE between 170-180°W (Rousselet et al. 2018) which could explain the relative increase in zooplankton biomass at SD-9. In general, the zooplankton biomass and abundance, and the taxonomic distribution vary from the center to the edge of an eddy whether it is cyclonic or anticyclonic in nature (Riandey et al. 2005), but the sampling resolution during OUTPACE did not allow us to

5   take into account this mesoscale variability.

The LD-B station was selected because of a large surface chl-*a* signal observed by satellite (de Verneil et al., 2017) for several weeks prior to sampling, and its sampling occurred at an advanced bloom stage with high N_2 fixation rates as the source of new production (Caffin et al., 2018a). Due to the late stage of this bloom when it was sampled, the potential physical processes that induced its formation cannot be definitively established (de Verneil et al. 2017). Chlorophyll

10   decreased sharply during the period of observation demonstrating a collapsing *Trichodesmium* bloom (Caffin et al, 2018a). Concomitantly, the abundance and taxonomic composition of zooplankton remained homogeneous in the water column. But the abundance of swimmers in the sediment traps decreased by half (Caffin et al, 2018a) suggesting an associated reduced zooplankton activity (production, vertical migration) not associated with high mortality. In contrast, the abundance and biomass of zooplankton in the ultra oligotrophic waters of the subtropical Pacific gyre (GY), were substantially lower than

15   the MA region (W-MA and CE-MA), linked to a far lower primary production mainly concentrated in a deeper chlorophyll maximum, 115–150m depth, in the GY waters (Van Wambeke et al 2018; Moutin et al, 2018), and associated with a reduced contribution of DDN.

The taxonomic structure found during OUTPACE (April-May) in the 4 zones (W-MA, CE-MA, BL and GY) showed a high degree of similarity in term of species richness and abundance distribution across the whole region. A moderate

20   difference was observed in the subtropical Pacific gyre (GY) where the copepod contribution to mesozooplankton was higher than in MA and LD-B, mostly in the small size classes (see our **Table 3**). In the W-MA and CE-MA, the sampling of teleost eggs and juveniles of euphausiaceae, although certainly under-sampled with our bongo net, indicated the presence of higher trophic levels in deeper waters in this region (Roger et al. 1994; Bertrand et al., 1999). In the Coral Sea, Rissik et al. (1997) and Smeti et al (2015) found similar taxonomic composition showing a relative stability in zooplankton composition,

25   despite spatial and temporal heterogeneity in environmental conditions. Our results suggest that this taxonomic stability in zooplankton assemblage remains valid for the extended WTSP. Interestingly, Dolan et al.'s (2016) analysis of the tintinnid ciliate community at stations LD-B and LD-C during OUTPACE found similar species richness, abundance distribution and size structure, with only the morphological diversity presenting some differences.

Data on the abundances and biomasses of mesozooplankton in the WTSP (**Table 7**) are scarcer than in the equatorial

30   waters (Le Borgne et al. 2011) and the eastern subtropical Pacific (Fernández-Álamo & Färber-Lorda, 2006). **Table 7** shows a general consistency between all these data for the tropical area, although variations could be discussed with respect to sampling season, regional spatio-temporal physical patterns, and sampling methods. Our data in the Coral Sea are comparable to those of Smeti et al. (2015), and Le Borgne et al. (1985, 2011), obtained at different seasons in oceanic waters around New Caledonia. Smeti et al. (2015) observed that the stations situated between New Caledonia and the Loyauté

Islands registered the highest abundance and biomass values during the cold season, but also the largest variations between stations. Around Mahé, Le Borgne et al (1985) found values ranging from 2.5 to 7 mg DW m^{-3}. In contrast, Le Borgne et al. (2011) found slightly lower biomass values than those observed during OUTPACE for oceanographic stations situated nearer to New Caledonia. All of these results highlight that the various mesoscale structures linked to flow disturbance in these oligotrophic bodies of water such as the Coral Sea have a significant effect on the distribution and abundance of zooplankton, imparting substantial heterogeneity, while also being the main seasonal driver of productivity in the region (Menkes et al., 2015; Smeti et al., 2015). On the eastern side of the OUTPACE transect, few data between 120-140°W, near the Marquesas Islands, give comparable low biomass levels (2 to 2.5 mg DW m^{-3}; BIOSOPE survey – Table 7). During the EastroPac cruise at the latitudes 20°N-20°S and longitude 110°W, Longhurst (1976) found abundance values ranging between 100 and 900 indm^{-3}, similarly to our observations. He noted that copepods were the dominant taxa, followed by chaetognaths and euphausiids. Between these two ends of the OUTPACE transect, no data were found for comparison with our observations. The obvious increased abundance and biomass in the MA (W-MA and CE-MA) region compared to the GY region is linked to waters of the Melanesian Archipelago being enriched by contact with multiple islands compared to the ultra-oligotrophic characteristics of the gyre (Rousselet et al.2018).There is somehow more information on zooplankton biomass and abundance in the Equatorial Pacific collected during the JGOFS program (Murray et al. 1995 and Le Borgne &Landry (2003). Le Borgne et al. (1999) studied the zonal variability of zooplankton and particle export in April-May 1996 in the Equatorial Pacific upwelling between 165° E and 150° W. This parallel transect to OUTPACE showed a general decreasing trend of zooplankton biomass from 14.4 mg DW m^{-3} at the eastern end to 8 mg DW m^{-3} at the western end (Le Borgne et al., 1999, their Fig.3) which was associated with a decrease of Chl-a. Almost all studies comparing zooplankton biomass sampled from the equator towards the tropic also show a strong zooplankton decrease parallel to decrease of Chl-a (Ikeda, 1985, his fig 3B; Dai et al. 2016; White et al., 1995; Fernández-Álamo& Färber-Lorda, 2006; Le Borgne et al, 2003).

4.3 Zooplankton association with diazotrophs

The OUTPACE transect was undertaken in a region known for its high N$_2$ fixation (Dupouy et al., 2011) which can contribute 30–50% of new production (Karl et al. 2002). During austral summer conditions, the Melanesian archipelago (New Caledonia, Vanuatu, Fiji Islands; Niué Island, our W-MA and CE-MA regions) is known for its recurrent large *Trichodesmium* blooms which dominates the diazotroph community (Bonnet et al., 2015), complemented by high abundances of UCYN-B (Bonnet et al., 2015; Moisander et al., 2010). During OUTPACE, very high values of N$_2$ fixation were registered in most of the W-MA and CE-MA stations, particularly in the upper 25 m, with a slight decrease at SD-9 and SD-10 (Bonnet et al, 2018, their Fig 2.e). Conversely, in the GY region, the N$_2$ fixation rates dropped to much lower values, with maximum levels occurring deeper in the water column (~50-60 m). In the W-MA and CE-MA regions, N$_2$ fixation was mainly attributed to high concentrations of *Trichodesmium* and to a lesser extent UCYN-B (Stenegren et al, 2018; Caffin et al, 2018a), and contributed circa 8-12 % of primary production (Caffin et al, 2018a). In the GY region, heterotrophic proteobacteria and UCYN-A types were responsible for N$_2$ fixation (Stenegren et al, 2017), and the N$_2$ fixation contribution

to primary production fell to 3 % (Caffin et al, 2018a). Up to recently, *Trichodesmium* were thought to be grazed by relatively few mesozooplankton species (Carpenter et al. 1999; Conroy et al., 2017), although new molecular techniques to detect diazotrophs in zooplankton gut contents are extending this list (Scavotto et al., 2015; Azimuddin et al. 2016; Hunt et al. 2016; Conroy et al. 2017). Such analyses were not performed during OUTPACE, and we limit our discussion to the observed correlations of key zooplankton species distribution with diazotroph distributions, particularly those among the top 10 species with respect to frequency of abundance (**Table 4).**

An abundant diazotroph community is expected to change the structure of the ecosystem, particularly the relative abundance and species composition of grazers and microbial population. The strong relationship found between *Trichodesmium* and zooplankton community spatial structuration during OUTPACE (BEST analysis) was characterized by positive correlations with the Harpacticoid copepods *M. gracilis* and *Miracia efferata* and the Poecilostomatoid copepod *Oncaea*. The association of *M. gracilis* with the colonial cyanobacterium *Trichodesmium* has been shown in several studies. This has been interpreted as reflecting a successful way of living within the plankton using filaments as a physical substrate for juvenile development and/or as a food source, and facilitated by *M. gracilis* being immune to cyanobacterial toxins harmful to other species of copepods (O'Neil and Roman, 1994; Eberl and Carpenter, 2007). A relationship between *Oncaea* and *Trichodesmium* was previously suggested by Dupuy et al (2016) in the Indian Ocean around Madagascar, based on stable isotope data. However, we found no significant relationship for *Pleuromamma* and *Euchaeta*, despite their association with *Trichodesmium* observed by Azimuddin et al (2016) in the western Pacific, nor for *Corycaeus*. It is worth noting that we found a positive correlation between pteropods (Thecosomata) and *Trichodesmium*, with decreasing abundance of this zooplankton group in GY compared to the other zones. Pteropods where in the top ten rank taxa in each zone, representing 1 to 10% of the total zooplankton abundance in the water column and up to 35% of the swimmers in the sediment traps (see Fig 7 A and B for comparison). As far as we are aware, a direct trophic link between Pteropods and *Trichodesmium* has never been established.

In the present study, we did not consider a possible association between zooplankton taxa and non-*Trichodesmium* diazotrophs but Hunt et al (2016) provided evidence for direct ingestion and assimilation of UCYN-C-derived N by the zooplankton from $^{15}N_2$ labelled grazing experiments. Recent observations suggested consumption of UCYN-A and UCYN-B by diverse calanoid copepods (Scavotto et al., 2015; Conroy et al., 2017). From the quantification of DDN to zooplankton $\delta^{15}N$ values, we estimated that DDN contributed up to 67 and 75% to zooplankton biomass in the W-MA and CE-MA regions respectively, but strongly decreased to an average of 22% in the GY region and dopwn to 7% in the eastern most station. Thus, the highest contribution of diazotrophic microorganisms to zooplankton occurred in the region of highest N_2 fixation and when *Trichodesmium* dominated the diazotrophs (74 to 100% in W-MA and CE-MA regions), whereas UCYN-B showed higher biomass in the GY region (37-86%). This is consistent with Caffin et al. (2018b) who showed that at the ecosystem level, even if the DDN transfer efficiency to zooplankton from UCYN-B (15 %) is higher from *Trichodesmium*, the quantity of DDN ultimately transferred to secondary producers is higher when *Trichodesmium* dominates, as cell-specific N_2 fixation rates of *Trichodesmium* are far higher than those of UCYN-B. The highest values of ZDDN were comparable

with the highest value (73%) observed during the VAHINE mesocosm experiment in the oligotrophic New Caledonia lagoon (Hunt et al. 2016), associated with a mixed diazotroph community of UCYN-C, *Trichodesmium* spp., and DDA (*Richelia* associated with the diatoms *Rhizosolenia* and *Hemiaulus* at lower concentrations).

4.4. Fluxes associated with zooplankton

The estimated weight specific rates of ingestion and NH_4 and PO_4 excretion from the relationships of Ikeda (1985) were found to be quite stable within and between regions and their ranges were fully consistent with literature values for metazooplankton and copepods in the inter-tropical zone (Ikeda, 1985; Dam et al, 1995; Mauchline, 1998; Hernández-León et al, 2008; McKinnon et al, 2015).The estimated ingestion and metabolic rates allowed us to estimate that the top-down (through grazing) and bottom-up impacts of zooplankton (through excretion of N and P) on phytoplankton were potentially high in the OUTPACE zone. Zooplankton grazing represented a daily removal of 6 to 27% of the phytoplankton stock and of 19 to 184% of the primary production. The top-down impact of mesozooplankton was higher than 50% of the daily primary production in CE-MA, BL and GY, with particularly high values in the CE-MA zone (up to 184%), but fell to 34% in the W-MA region. In general, for all regions, our estimated mesozooplankton grazing related to primary production values were in the upper range of the global comparative analysis by Calbet (2001, his Fig. 1) suggesting a strong top-down pressure by zooplankton. During OUTPACE this pressure was mainly exerted on nano- and microphytoplankton (see our Table 6). The grazing impact on picoplankton was probably exerted by microzooplankton which also displayed high abundances in this area (Dolan, et al., 2016). As a whole, this grazing process may lead to an equilibrium between phytoplankton production and grazing by mesozooplankton as observed in the equatorial Pacific (Landry et al., 2001). From our results, we can also estimate that the top down impact of zooplankton on N_2 fixers must be important. Indeed, Caffin et al (2018a, 2018b) estimated that N_2 fixation contributed circa 8-12 % of primary production in the MA region and 3 % in the GY water and sustained nearly all new primary production at all stations. As zooplankton grazing removed 19 to 184% of the total primary production daily, we can estimate that 1.5 to 22 % of N_2fixing organisms were removed daily. At the long duration stations, the fecal pellet production was estimated to be 71, 128, and 31 mg C m^{-2} d^{-1} for LD-A, LD-B and LD-C respectively, considering an assimilation efficiency of 0.7 on the ZCD_H (see Table 6). These values are much higher than measured mean values of particle vertical export of 27.1, 3.5 and 3.8 mg C m^{-2} d^{-1} respectively for the same stations (Caffin et al.2018). This would mean that only a very small percentage of zooplankton fecal pellets are collected in sediment traps, and could partly explain the disequilibrium between new and export production observed by Caffin et al (2018).

Regeneration of nutrients by zooplankton excretion was high suggesting a high contribution to regenerated production particularly in terms of nitrogen. Valdes et al (this issue) demonstrated that copepod metabolism (mainly excretion) can provide substantial amounts of ammonium, dissolved organic nitrogen (DON) and dissolved organic phosphorus (DOP) in the WTSP, which microbial communities can directly use in short response time enhancing bacterioplankton remineralization. Daily NH_4 excretion represented 14.5 to 165 % of phytoplankton needs for N whereas PO_4 excretion accounted for only 2.8 to 34 of P needs. These estimates for NH_4 regeneration are in the upper range of literature data

summarized by Hernández-León et al (2008) and Le Borgne (1986) for different areas of the world ocean, and higher than those reported for the central tropical Pacific (up to 17%; Dam et al, 1995; Zhang et al 1995), the equatorial Pacific (31–36%; Gaudy et al.; 2003) and for the North Pacific central gyre (40–50%; Eppley et al., 1973), but similar to values recorded in the Atlantic Ocean between 50°N and 30°S (31–100%; Isla et al., 2004). Our estimates of the contribution of phosphorous

5   excretion to phytoplankton requirements are also in the range of the literature values reviewed by Le Borgne et al. (1985). Ammonium is recognized as the primary nitrogenous excretory product of zooplankton. However, zooplankton can excrete substantial amount of organic nitrogen and phosphorus (DON and DOP), exceeding even the ammonium and phosphate excretion (Steinberg and Saba 2008). Thus, the impact of ammonia excretion of phytoplankton nitrogen demands could be substantially higher that our estimations and even more if we considered that zooplankton can contribute to the new and

10   regenerated production through different pathways such as the sloppy feeding and leaching from fecal pellets that was not determined in this study. In addition, the impact of zooplankton excretion is not limited tothe upper layers as zooplankton conduct diel vertical migrations through the water column. Thus, the impact of zooplankton metabolism (excretion and grazing) on biogeochemical fluxes could be much higher that we can estimate in this study and further studies are necessary to determine the fate of the different products derived from zooplankton metabolism in WTSP.

15   During OUTPACE, there was no clear spatial trend in top-down (grazing) vs bottom-up (N and P regeneration) zooplankton impacts on phytoplankton, although both processes appeared important in all sites. Finally, despite the relatively low biomass values of planktonic components in quasi-steady state, the availability of micro- and macronutrients related to physical mesoscale patterns in the waters surrounding the Melanesian archipelago, the fueling by DDN and the relatively high rates of plankton production may explain why it is the basis of a productive trophic chain ending with valuable

20   fisheries. This trophic link with upper trophic levels is realized through the process of zooplankton diel vertical migration and their predation by mesopelagic fish (Rissik& Suthers, 2000; Menkes et al. 2015).

The percentage of estimated zooplankton respiration rates relative to primary production (averaging 29% and 60% respectively, depending on the region, , see Table 6) were high but in the range of global depth-integrated values reported by Calbet (2001). The lower rate registered at the station west of the New Caledonia (7%, SD-1) was comparable to the 8%

25   measured by McKinnon et al. (2015) in the Great Barrier Reef waters, NE Australia. Our observations also clearly support diel vertical migration of zooplankton in the MA zone as epipelagic zooplankton biomass increased in night samples compared to day samples in LD-A and LD-B, with a contribution of all size-classes (see Fig.6). The migratory zooplankton biomasses estimated at the two stations were on the upper range of values observed at low latitudes (Le Borgne & Rodier, 1997; Steinberg et al., 2000). Consequently, the carbon flux associated with the respiration of migrants was also among the

30   highest values obtained in similar studies (see review by Steinberg et al, 2000), probably linked to the contribution of all size classes to the migrating biomass. Other contributions of the mesozoooplankton to the carbon flux through DOC excretion and mortality have not been evaluated in our study. The strong grazing impact on primary producers and the high metabolic losses, partly realized in mesopelagic waters due to diurnal migrations emphasize the role of zooplankton in the sink of

atmospheric CO_2 in tropical regions as underlined by Steinberg et al (2000), and hypothesized by Moutin et al (2018) in their carbon budget at the OUTPACE long term stations.

Finally, our estimations of the top down (ingestion) and bottom-up (excretion) impacts (expressed in percentages in Table 6) and of the fluxes (expressed in biomass per day in Table 6)associated with zooplankton were highly variable between stations and zones, but high in comparison to literature data in most cases (Hernández-León & Ikeda, 2005; Hernández-León et al. 2008). These high values can be attributed to high ingestion and metabolic rates in relation to the high contribution of small taxonomic forms in our samples (partly linked to the mesh of sampling - 120 μm mesh) and to our taxon-based calculation of rates (see methods).The highest values of phyto – and zooplankton biomasses and of primary production during OUTPACE were found at the boundary between the oligotrophic and ultra-oligotrophic regions (LD-B and LD-C). However, the grazing and excretion impacts of zooplankton on phytoplankton were very similar between the two zones, partly due to similar ratio of biomass to production, and to comparable specific ingestion and metabolic rates linked to similar community structures. In the MA zone, as plankton biomasses and community structure were rather stable, the high variability of the top down (ingestion) and bottom-up (excretion) impacts found in this area might be attributed to the high mesoscale activity, leading to temporal and spatial shifts between phytoplankton and zooplankton biomasses and productions.

.

Acknowledgements

This is a contribution of the OUTPACE (Oligotrophy from Ultra-oligoTrophyPACific Experiment) project funded by the French research National agency (ANR-14-CE01-0007-01), the LEFE-CyBER program (CNRS-INSU), the GOPS program (IRD) and the CNES (BC T23, ZBC 4500048836) and by European FEDER Fund under project 1166-39417 The

5   OUTPACE cruise (DOI: http://dx.doi.org/10.17600/15000900) was managed by T. Moutin and S. Bonnet from the MIO (Mediterranean Institute of Oceanography). The authors thank to the crew of the R/V L´Atalante for outstanding shipboard operation. This work was supported by the Comisión Nacional de Investigación Científicas y Tecnológicas (CONICYT) through Grants FONDECYT No 1130511 and 1150891 and Instituto Milenio de Oceanografía (IMO) Grant IC120019. Valdés and Donoso were funded by CONICYT Scholarship. Hunt was funded in part from the European Union's Seventh

10 Framework Programme for research, technological development and demonstration undergrant agreement no. 302010 – project ISOZOO. The authors thank France Van Wambeke, Cécile Dupouy and Marcus Stenegren and for sharing their data on primary production chlorophyll and diazotroph abundance (respectively), that helped for interpretation and comparison with our results. The authors thank both referees for their many constructive suggestions.

References

Azimuddin, K. M., Hirai, J., Suzuki, S., Haider, M. N., Tachibana, A., Watanabe, K., Kitamura, M., Hashihama, F., Takahashi, K. and Hamasaki, K.: Possible association of diazotrophs with marine zooplankton in the Pacific Ocean. Microbiology Open, 5(6), 1016-1026,doi: 10.1002/mbo3.385 , 2016.

5 Bertrand A., Le Borgne R. and Josse E.: Acoustic characterization of micronekton distribution in French Polynesia. Mar. Ecol.Prog. Ser., 191, 127–140. 1999

Bonnet, S., Biegala, I. C., Dutrieux, P., Slemons, L. O. and Capone, D. G.: Nitrogen fixation in the western equatorial Pacific: Rates, diazotrophic cyanobacterial size class distribution, and biogeochemical significance, Global Biogeochem. Cycles, 23(3), GB3012, doi:10.1029/2008GB003439, 2009.

10 Bonnet, S., Rodier, M., Turk-Kubo, K. A., Germineaud, C., Menkes, C., Ganachaud, A., Cravatte, S., Raimbault, P., Campbell, E., Quéroué, F., Sarthou, G., Desnues, A., Maes, C. and Eldin, G.: Contrasted geographical distribution of N2 fixation rates and nifHphylotypes in the Coral and Solomon Seas (southwestern Pacific) during austral winter conditions, Global Biogeochem. Cycles, 29(11), 2015GB005117, doi:10.1002/2015GB005117, 2015.

Bonnet, S., Caffin, M., Berthelot, H., and Moutin, T.: Hot spot of N2 fixation in the western tropical South Pacific pleads for

15 a spatial decoupling between N2fixation and denitrification, PNAS Letter, 114, E2800–E2801, doi/10.1073/pnas.1619514114, 2017.

Bonnet, S., Caffin, M., Berthelot, H., Grosso, O., Benavides, M., Helias-Nunige, S., Guieu, C., Stenegren, M., and Foster, R. A.: In-depth characterization of diazotroph activity across the western tropical South Pacific hotspot of N2 fixation (OUTPACE cruise), Biogeosciences, 15, 4215-4232, https://doi.org/10.5194/bg-15-4215-2018, 2018.

20 Buitenhuis, E. T., Li, W. K. W., Vaulot, D., Lomas, M. W., Landry, M. R., Partensky, F., Karl, D. M., Ulloa, O., Campbell, L., Jacquet, S., Lantoine, F., Chavez, F., Macias, D., Gosselin, M. and McManus, G. B.: Picophytoplankton biomass distribution in the global ocean, Earth System Science Data, 4(1), 37–46, 2012.

Caffin, M., Moutin, T., Foster, R. A., Bouruet-Aubertot, P., Doglioli, A. M., Berthelot, H., Guieu, C., Grosso, O., Helias-Nunige, S., Leblond, N., Gimenez, A., Petrenko, A. A., de Verneil, A., and Bonnet, S.: N$_2$ fixation as a dominant new N

25 source in the western tropical South Pacific Ocean (OUTPACE cruise), Biogeosciences, 15, 2565-2585, https://doi.org/10.5194/bg-15-2565-2018, 2018a.

Caffin, M., Berthelot, H., Cornet-Barthaux, V., Barani, A., and Bonnet, S.: Transfer of diazotroph-derived nitrogen to the planktonic food web across gradients of N$_2$ fixation activity and diversity in the western tropical South Pacific Ocean, Biogeosciences, 15, 3795-3810, https://doi.org/10.5194/bg-15-3795-2018, 2018b.

30 Campbell, L., Carpenter, E. J., Montoya, J. P., Kustka, A. B. and Capone, D. G.: Picoplankton community structure within and outside a *Trichodesmium* bloom in the southwestern Pacific Ocean, Vie et milieu, 55(3–4), 185–195, 2005.

Carpenter, E. J., Montoya J. P., Burns J., Mulholland M. R., Subramaniam A., and Capone D. G.:Extensivebloom of a N2-fixing diatom/cyanobacterial association in the tropical Atlantic Ocean. Mar. Ecol. Prog. Ser. 185:273–283, 1999.

Ceccarelli, D. M., McKinnon, A. D., Andrefouet, S., Allain, V., Young, J., Gledhill, D. C., Flynn, A., Bax, N. J., Beaman, R., Borsa, P., Brinkman, R., Bustamante, R. H., Campbell, R., Cappo, M., Cravatte, S., D'Agata, S., Dichmont, C. M., Dunstan, P. K., Dupouy, C., Edgar, G., Farman, R., Furnas, M., Garrigue, C., Hutton, T., Kulbicki, M., Letourneur, Y., Lindsay, D., Menkes, C., Mouillot, D., Parravicini, V., Payri, C., Pelletier, B., de Forges, B. R., Ridgway, K., Rodier, M., Samadi, S., Schoeman, D., Skewes, T., Swearer, S., Vigliola, L., Wantiez, L., Williams, A., Williams, A., and Richardson, A. J.: Chapter IV : The Coral Sea: Physical Environment, Ecosystem Status and Biodiversity Assets. In Michael Lesser, editor: Advances in Marine Biology, Vol. 66, AMB, UK: Academic Press, pp. 213-290

Conroy, B. J., Steinberg, D. K., Song, B., Kalmbach, A., Carpenter, E. J. and Foster, R. A.: Mesozooplankton Graze on Cyanobacteria in the Amazon River Plume and Western Tropical North Atlantic, Frontiers in Microbiology, 8, doi:10.3389/fmicb.2017.01436, 2017.

Conway, D. V., White, R. G., Hugues-Dit-Ciles, J., Gallienne, C. P. and Robins, D. B.: Guide to the coastal and surface zooplankton of the south-western Indian Ocean. Occasional Publication of the Marine Biological Association 15, 2003.

Dai, L. P., Li, C. L., Yang, G., and Sun, X. X.: Zooplankton abundance, biovolume and size spectra at western boundary currents in the subtropical North Pacific during winter 2012, Journal of Marine Systems, 155, 73-83, 10.1016/j.jmarsys.2015.11.004, 2016.

Dam, H. G., Roman, M. R. and Youngbluth, M. J.: Downward export of respiratory carbon and dissolved inorganic nitrogen by diel-migrant mesozooplankton at the JGOFS Bermuda time-series station, Deep-Sea Res. Pt. I, 42(7), 1187–1197, doi:10.1016/0967-0637(95)00048-B, 1995.

deVerneil, A., Rousselet, L., Doglioli, A. M., Petrenko, A. A., Maes, C., Bouruet-Aubertot, P., and Moutin, T.: OUTPACE long duration stations: physical variability, context of biogeochemical sampling, and evaluation of sampling strategy, Biogeosciences, 15, 2125-2147, https://doi.org/10.5194/bg-15-2125-2018, 2018.

deVerneil, A., Rousselet, L., Doglioli, A. M., Petrenko, A. A., and Moutin, T.: The fate of a southwest Pacific bloom: gauging the impact of submesoscale vs. mesoscale circulation 780 on biological gradients in the subtropics, Biogeosciences, 14, 3471–3486, doi.org/10.5194/bg-14-3471-2017, 2017.

Dolan, J. R., Gimenez, A., Cornet-Barthaux, V., and Verneil, A.: Community Structure of Tintinnid Ciliates of the Microzooplankton in the South West Pacific Ocean: Comparison of a High Primary Productivity with a Typical Oligotrophic Site, Journal of Eukaryotic Microbiology, 63, 813-822, 2016.

Donoso, K., Carlotti, F., Pagano, M., Hunt, B. P. V., Escribano, R. and Berline, L.: Zooplankton community response to the winter 2013 deep convection process in the NW Mediterranean Sea, J. Geophys. Res.-Oceans.,122 (3), 2319-2338, doi:10.1002/2016JC012176, 2017.

Dupouy, C., Benielli-Gary, D., Neveux, J., Dandonneau, Y. and Westberry, T. K.: An algorithm for detecting Trichodesmium surface blooms in the South Western Tropical Pacific, Biogeosciences, 8(12), 3631–3647, doi:10.5194/bg-8-3631-2011, 2011.

Dupouy, C., Frouin, R., Tedetti, M., Maillard, M., Rodier, M., Lombard, F., Guidi, L., Picheral, M., Duhamel, S., Charrière, B., and Sempéré, R.: DiazotrophicTrichodesmium influence on ocean color and pigment composition in the South West tropical Pacific, Biogeosciences Discuss., https://doi.org/10.5194/bg-2017-570, in review, 2018.

Dupuy, C., Pagano, M., Got, P., Domaizon, I., Chappuis, A., Marchessaux, G. and Bouvy, M.: Trophic relationships between metazooplankton communities and their plankton food sources in the Iles Eparses (Western Indian Ocean), Mar. Environ. Res., 116, 18–31, doi:10.1016/j.marenvres.2016.02.011, 2016.

Eberl, R., and Carpenter, E. J.: Association of the copepod *Macrosetella gracilis* with the cyanobacterium *Trichodesmium* spp. in the North Pacific Gyre, Mar. Ecol.Prog. Ser., , 333, 205-212, 2007.

Eppley, R. W., Renger, E. H., Venrick, E. L. and Mullin, M. M.: A study of plankton dynamics and nutrient cycling in the central gyre of the North Pacific Ocean, Limnol. Oceanogr., 18(4), 534–551, 1973.

Fernández-Álamo, M. A. and Färber-Lorda, J.: Zooplankton and the oceanography of the eastern tropical Pacific: A review, Prog. Oceanogr., 69(2–4), 318–359, doi:10.1016/j.pocean.2006.03.003, 2006.

Gaudy, R., Champalbert, G., Le Borgne, R., : Feeding and metabolism of mesozooplankton in the equatorial Pacific high-nutrient, low-chlorophyll zone along 180 . J. Geophys. Res.-Oceans.,108 (C12), 8144., 2003

Gorsky, G., Ohman, M. D., Picheral, M., Gasparini, S., Stemmann, L., Romagnan, J. B., Cawood, A., Pesant, S., Pesant, C., and Prejger, F.: Digital zooplankton image analysis using the ZooScan integrated system, J. Plankton Res., 32, 285–303, 2010.

Grosjean, P., Picheral, M., Warembourg, C. and Gorsky, G.: Enumeration, measurement, and identification of net zooplankton samplesusing the ZOOSCAN digital imaging system, ICES J. Mar. Sci., 61(4), 518–525, 2004.

Hawser, S. P., O'Neil, J. M., Roman, M. R. and Codd, G. A.: Toxicity of blooms of the cyanobacterium *Trichodesmium* to zooplankton, J ApplPhycol, 4(1), 79–86, doi:10.1007/BF00003963, 1992.

Hernández-León, S., Fraga, C. and Ikeda, T.: A global estimation of mesozooplankton ammonium excretion in the open ocean, J Plankton Res, 30(5), 577–585, doi:10.1093/plankt/fbn021, 2008.

Houssard, P., Lorrain, A., Tremblay-Boyer, L., Allain, V., Graham, B. S., Menkes, C. E., Pethybridge, H., Couturier, L. I. E., Point, D., Leroy, B., Receveur, A., Hunt, B. P. V., Vourey, E., Bonnet, S., Rodier, M., Raimbault, P., Feunteun, E., Kuhnert, P. M., Munaron, J.-M., Lebreton, B., Otake, T. and Letourneur, Y.: Trophic position increases with thermocline depth in yellowfin and bigeye tuna across the Western and Central Pacific Ocean, Prog. Oceanogr., 154, 49–63, doi:10.1016/j.pocean.2017.04.008, 2017.

Hunt, B. P. V., Allain, V., Menkes, C., Lorrain, A., Graham, B., Rodier, M., Pagano, M. and Carlotti, F.: A coupled stable isotope-size spectrum approach to understanding pelagic food-web dynamics: A case study from the southwest sub-tropical Pacific, Deep-Sea Res. Pt. II, 113, 208–224, doi:10.1016/j.dsr2.2014.10.023, 2015.

Hunt, B. P. V., Bonnet, S., Berthelot, H., Conroy, B. J., Foster, R. A. and Pagano, M.: Contribution and pathways of diazotroph-derived nitrogen to zooplankton during the VAHINE mesocosm experiment in the oligotrophic New Caledonia lagoon, Biogeosciences, 13(10), 3131–3145, doi:10.5194/bg-13-3131-2016, 2016.

Ikeda, T.: Metabolic rates of epipelagic marine zooplankton as a function of body mass and temperature, Marine Biology, 85(1), 1–11, 1985.

Isla, J. A., Llope, M. and Anadón, R.: Size-fractionated mesozooplankton biomass, metabolism and grazing along a 50 N-30 S transect of the Atlantic Ocean, J Plankton Res, 26(11), 1301–1313, 1985

5 Karl, D., Michaels, A., Bergman, B., Capone, D., Carpenter, E., Letelier, R., Lipschultz, F., Paerl, H., Sigman, D., and Stal L.: Dinitrogen fixation in the world's oceans. In: The Nitrogen Cycle at Regional to Global Scales, Boyer, E. W. and Howarth, R. W. (Eds.), Springer, Dordrecht, 47-98, 2002

Kiørboe T., MohlenbergF.and Hamburger K. Bioenergetics of the planktonic copepod *Acartiatonsa*: relation between feeding, egg production and respiration, and composition of specific dynamic action. Mar. Ecol.Prog. Ser., 26, 85-97, 1985

10 Landry, M. R., Al-Mutairi, H., Selph, K. E., Christensen, S. and Nunnery, S.: Seasonal patterns of mesozooplankton abundance and biomass at Station ALOHA, Deep-Sea Res. Pt. II, 48(8), 2037–2061, 2001.

Le Borgne, R.:The release of soluble end products of metabolism. In Corner, E. D. S. and O'Hara, S. C. M. (eds), The BiologicalChemistry of Marine Copepods. Clarendon, pp. 109–164.,1986

Le Borgne, R., Dandonneau, Y. and Lemasson, L.: The problem of the island mass effect on chlorophyll and zooplankton

15 standing crops around Mare (Loyalty Islands) and New Caledonia, Bulletin of Marine Science, 37(2), 450–459, 1985.

Le Borgne, R. and Rodier, M.: Net zooplankton and the biological pump: a comparison between the oligotrophic and mesotrophic equatorial Pacific, Deep-Sea Res. Pt. II,,, 44(9), 2003–2023, doi:10.1016/S0967-0645(97)00034-9, 1997.

Le Borgne, R., Rodier, M., Le Bouteiller, A. and Murray, J. W.: Zonal variability of plankton and particle export flux in the equatorial Pacific upwelling between 165 E and 150 W, OceanologicaActa, 22(1), 57–66, 1999.

20 Le Borgne, R., Feely, R. A. and Mackey, D. J.: Carbon fluxes in the equatorial Pacific: a synthesis of the JGOFS programme, Deep-Sea Res. Pt. II,,, 49(13), 2425–2442, doi:10.1016/S0967-0645(02)00043-7, 2002.

Le Borgne, R., Champalbert, G. and Gaudy, R.: Mesozooplankton biomass and composition in the equatorial Pacific along 180°, .J. Geophys. Res.-,, 108(C12), doi:10.1029/2000JC000745, 2003.

Le Borgne, R. and Landry, M. R.: EBENE: A JGOFS investigation of plankton variability and trophic interactions in the

25 equatorial Pacific (180°), J. Geophys. Res., 108(C12), 8136, 2003.

Le Borgne, R., Douillet, P., Fichez, R. and Torréton, J.-P.: Hydrography and plankton temporal variabilities at different time scales in the southwest lagoon of New Caledonia: A review, Marine Pollution Bulletin, 61(7–12), 297–308, doi:10.1016/j.marpolbul.2010.06.022, 2010.

Le Borgne, R., Allain V., Matear R. J., Griffiths S. P., McKinnon A. D., Richardson A. J., and Young J. W.:Vulnerability of

30 open ocean food webs in the tropical Pacific to climate change, in Vulnerability of Fisheries and Aquaculture in the Tropical Pacific to Climate Change, edited by J. Bell, J. E. Johnson, and A. J. Hobday, Secr. of the Pac. Community, Noumea, 2011.

Lehette, P. and Hernández-León, S.: Zooplankton biomass estimation from digitized images: a comparison between subtropical and Antarctic organisms, Limnol. Oceanogr.: Methods, 7, 304–308, 2009.

Longhurst A. R.: Interactions between zooplankton and phytoplankton profiles in the eastern tropical Pacific Ocean. Deep-Sea Res., 23, 729–754, 1976.

Longhurst, A. R.: Ecological Geography of the Sea. Academic Press, San Diego, Calif, 560 p., 2006.

McCutchan, J.H., Lewis, W.M., Kendall, C., McGrath, C.C.:Variation in trophic shift for stable isotope ratios of carbon, nitrogen, and sulfur. Oikos 102, 378-390, 2003.

McKinnon A.D., Doyle J., Duggan S., Logan M., Lønborg C. and Brinkman R.: Zooplankton Growth, Respiration and Grazing on the Australian Margins of the Tropical Indian and Pacific Oceans. PLoS ONE 10(10): e0140012ttps://doi.org/10.1371/journal.pone.0140012, 2015.

Mauchline, J.:The Biology of Calanoid Copepods. Advances in Marine Biology 33: 1-710, 1998.

Menkes, C. E., Allain, V., Rodier, M., Gallois, F., Lebourges-Dhaussy, A., Hunt, B. P. V., Smeti, H., Pagano, M., Josse, E., Daroux, A., Lehodey, P., Senina, I., Kestenare, E., Lorrain, A. and Nicol, S.: Seasonal oceanography from physics to micronekton in the south-west Pacific, Deep-Sea Res. Pt. II, 113, 125–144, doi:10.1016/j.dsr2.2014.10.026, 2015.

Moisander, P. H., Beinart, R. A., Hewson, I., White, A. E., Johnson, K. S., Carlson, C. A., Montoya, J. P. and Zehr, J. P.: Unicellular Cyanobacterial Distributions Broaden the Oceanic N2 Fixation Domain, Science, 327(5972), 1512–1514, doi:10.1126/science.1185468, 2010.

Montoya, J. P., Carpenter, E. J. and Capone, D. G.: Nitrogen fixation and nitrogen isotope abundances in zooplankton of the oligotrophic North Atlantic, Limnol. Oceanogr., 47(6), 1617–1628, doi:10.4319/lo.2002.47.6.1617, 2002.

Moutin, T., Doglioli, A. M., de Verneil, A. and Bonnet, S.: Preface: The Oligotrophy to the UlTra-oligotrophy PACific Experiment (OUTPACE cruise, 18 February to 3 April 2015), Biogeosciences, 14(13), 3207–3220, doi:10.5194/bg-14-3207-2017, 2017.

Moutin, T., Wagener, T., Caffin, M., Fumenia, A., Gimenez, A., Baklouti, M., Bouruet-Aubertot, P., Pujo-Pay, M., Leblanc, K., Lefevre, D., HeliasNunige, S., Leblond, N., Grosso, O., and de Verneil, A.: Nutrient availability and the ultimate control of the biological carbon pump in the western tropical South Pacific Ocean, Biogeosciences, 15, 2961-2989, https://doi.org/10.5194/bg-15-2961-2018, 2018.

Murray, J. W., Johnson, E., and Garside, C.: A U.S. JGOFS process study in the equatorial Pacific (EqPac): Introduction, Deep-Sea Res. Pt. II, 42, 275–293, 1995.

Nival, P., Nival, S. and Thiriot, A.: Influence des conditions hivernales sur les productions phyto-et zooplanctoniques en Méditerranée Nord-Occidentale. V. Biomasse et production zooplanctonique—relations phyto-zooplancton, Marine Biology, 31(3), 249–270, 1975.

O'Neil, J. M.: The colonial cyanobacterium *Trichodesmium* as a physical and nutritional substrate for the harpacticoid copepod *Macrosetella gracilis*, J Plankton Res, 20(1), 43–59, doi:10.1093/plankt/20.1.43, 1998.

O'Neil, J. M. and Roman, M. R.: Ingestion of the *Trichodesmium* spp. by pelagic harpacticoid copepods *Macrosetella, Miracia* and *Oculosetella*, in Ecology and Morphology of Copepods, pp. 235–240, Springer, Dordrecht., 1994.

Razouls, C., F. De Bovée, J. Kouwenberg, and Desreumaux: Diversity and geographic distribution of marine planktonic copepods, http://copepodes.obs-banyuls.fr/en, 2005-2017.

Riandey, V., Champalbert, G., Carlotti, F., Taupier-Letage, I., and Thibault-Botha, D.: Zooplankton distribution related to the hydrodynamic features in the Algerian Basin (western Mediterranean Sea) in summer 1997, Deep-Sea Res. Pt. I, 52, 2029–2048, 2005.

Rissik, D., Suthers, I. M., and Taggart, C. T.: Enhanced zooplankton abundance in the lee of an isolated reef in the south Coral Sea: the role of flow disturbance, Journal of Plankton Research, 19, 1347-1368, 1997.

Rissik, D., and Suthers, I. M.: Enhanced feeding by pelagic juvenile myctophid fishes within a region of island-induced flow disturbance in the Coral Sea, Mar. Ecol. Prog. Ser., 203, 263-273, 2000.

Roger, C.: Relationships among yellowfin and skipjack tuna, their prey-fish and plankton in the tropical western Indian Ocean, Fisheries Oceanography, 3(2), 133–141, doi:10.1111/j.1365-2419.1994.tb00055.x, 1994.

Rose, M.: Copépodes pélagiques. Faune de France 26. Edit. P. Lechevalier Paris,374p.,1933.

Rousselet, L., de Verneil, A., Doglioli, A. M., Petrenko, A. A., Duhamel, S., Maes, C., and Blanke, B.: Large- to submesoscale surface circulation and its implications on biogeochemical/biological horizontal distributions during the OUTPACE cruise (southwest Pacific), Biogeosciences, 15, 2411-2431, https://doi.org/10.5194/bg-15-2411-2018, 2018.

Sarmiento, J. L. and Gruber, N.: Ocean Biogeochemical Dynamics,Princeton University Press, Princeton, New Jersey, 2006.

Scavotto, R. E., Dziallas, C., Bentzon-Tilia, M., Riemann, L., and Moisander, P. H.. Nitrogen-fixing bacteria associated with copepods in coastal waters ofthe North Atlantic Ocean. Environ. Microbiol. 17, 3754–3765. doi: 10.1111/1462-2920.12777, 2015.

Shannon, C. E., and Weaver, G.: The Mathematical Theory of Communication, Univ. of Ill. Press, Urbana. 1949

Shiozaki, T., Kodama, T. and Furuya, K.: Large-scale impact of the island mass effect through nitrogen fixation in the western South Pacific Ocean, Geophysical Research Letters, 41(8), 2907–2913, doi:10.1002/2014GL059835, 2014.

Smeti, H., Pagano, M., Menkes, C., Lebourges-Dhaussy, A., Hunt, B. P. V., Allain, V., Rodier, M., de Boissieu, F., Kestenare, E. and Sammari, C.: Spatial and temporal variability of zooplankton off New Caledonia (Southwestern Pacific) from acoustics and net measurements, J. Geophys. Res.-Oceans.,, 120(4), 2676–2700, doi:10.1002/2014JC010441, 2015.

Sommer, S., Hansen, T. and Sommer, U :Transfer of diazotrophic nitrogen to mesozooplankton in Kiel Fjord, Western Baltic Sea: a mesocosm study. Mar. Ecol. Prog. Ser. 324, 105-112, 2006.

Stenegren, M., Caputo, A., Berg, C., Bonnet, S., and Foster, R. A.: Distribution and drivers of symbiotic and free-living diazotrophic cyanobacteria in the western tropical South Pacific, Biogeosciences, 15, 1559-1578, https://doi.org/10.5194/bg-15-1559-2018, 2018.

Steinberg, D. K., Carlson, C. A., Bates, N. R., Goldthwait, S. A., Madin, L. P., and Michaels, A. F.: Zooplankton vertical migration and the active transport of dissolved organic and inorganic carbon in the Sargasso Sea, Deep-Sea Res. Pt. I, 47, 137–158, 2000.

Steinberg, D. K., and Saba, G. K.: "Nitrogen consumption and metabolism in marine zooplankton," in Nitrogen in the Marine Environment, ed D. G. Capone (Boston: Academic Press), 1135–1196,2008

Tregouboff, G., and Rose M.: Manuel de Planctonologie Méditerranéenne, tome II Centre National de la Recherche Scientifique Paris, Tomes I et II, 1-181, 1957.

5   Turner, J. T.: Planktonic marine copepods and harmful algae, Harmful Algae, 32, 81–93, doi:10.1016/j.hal.2013.12.001, 2014.

Valdés, V., Carlotti, F., Escribano, R., Donoso, K., Pagano, M., Molina, V., and Fernandez, C.: Nitrogen and phosphorus recycling mediated by copepods in Western Tropical South Pacific, Biogeosciences Discuss., https://doi.org/10.5194/bg-2017-563, in review, 2018.

10   Vanderklift, M.A. and Ponsard, S.,: Sources of variation in consumer-diet δ15N enrichment: a meta-analysis. Oecologia V136, 169-182. 2003

Van Wambeke, F., Duhamel, S., Gimenez, A., Lefèvre, D., Pujo- Pay, M., and Moutin, T.: Dynamics of phytoplankton and heterotrophic bacterioplankton in the Western Tropical South Pacific Ocean along a gradient of diversity and activity of diazotrophs, Biogeosciences, 2018.

15   Weber, S. C., Carpenter, E. J., Coles, V. J., Yager, P. L., Goes, J. and Montoya, J. P.: Amazon River influence on nitrogen fixation and export production in the western tropical North Atlantic: Amazon River influence on nitrogen fixation, Limnol. Oceanogr., 62(2), 618–631, doi:10.1002/lno.10448, 2017.

White, J. R., Zhang, X., Welling, L. A., Roman, M. R. and Dam, H. G.: Latitudinal gradients in zooplankton biomass in the tropical Pacific at 140°W during the JGOFS EqPac study: Effects of El Niño, Deep-Sea Res. Pt. II, 42(2), 715–733,
20   doi:10.1016/0967-0645(95)00033-M, 1995.

Wirtz K.W.: Who is eating whom? Morphology and feeding type determine the size relations between planktonic predators and their ideal prey. Mar. Ecol. Prog. Ser., 445, 1–12, 2012.

Zehr, J. P., Waterbury, J. B., Turner, P. J., Montoya, J. P., Omoregie, E., Steward, G. F., Hansen, A. and Karl, D. M.: Unicellular cyanobacteria fix N_2 in the subtropical North Pacific Ocean, Nature, 412(6847), 635, doi:10.1038/35088063,
25   2001.

Zhang, X., Dam, H. G., White, J. R. and Roman, M. R.: Latitudinal variations in mesozooplankton grazing and metabolism in the central tropical Pacific during the U.S. JGOFS EqPac study, Deep-Sea Res. Pt. II, 42(2), 695–714, doi:10.1016/0967-0645(95)00032-L, 1995

Zhou, M., Carlotti, F. and Zhu, Y.: A size-spectrum zooplankton closure model for ecosystem modelling, Journal of
30   Plankton Research, 32(8), 1147–1165, doi:10.1093/plankt/fbq054, 2010.

Table 1. Mean values (± standard deviation) of salinity (‰), temperature (°C), total Chl-*a* and Phae (µg L^{-1}), % Chl-*a*, and MLD depth (m) found at the stations for the four clusters defined in the PCA analysis on environmental variables (see Fig.1) and for the 3 long duration stations. W-MA = Western Melanesian archipelago, CE-MA= Central and Eastern Melanesian archipelago, BL = station B (blooming conditions) and GY = subtropical gyre. Letters below the mean values indicate

5 homogeneous groups between zones (small letters) or LD stations (cap letters) according to post hoc Scheffé tests.

	W-MA	CE-MA	BL	GY	LD-A	LD-B	LD-C
MLD	14.69 ± *4.46*	15.67 ± *5.34*	26.75	34.25 ± *5.63*	16.75 ± 5.56	26.75 ± 6.13	28.75 ± 9.52
	a	a	ab	b	A	A	A
Salinity	35.27 ± *0.41*	35.58 ± *0.03*	36.31	35.86 ± *0.30*	35.43 ± 0.07	36.31 ± 0.48	36.19 ± 0.57
	a	ab	b	b	A	A	A
Temperature	24.59 ± *0.78*	23.95 ± *0.65*	25.38	25.36 ± *0.36*	25.38 ± 0.63	25.38 ± 0.45	24.96 ± 0.68
	ab	a	ab	b	A	A	A
Chla + Phae	0.42 ± *0.06*	0.38 ± *0.09*	0.48	0.19 ± *0.04*	0.42 ± 0.07	0.48 ± 0.10	0.23 ± 0.02
	a	a	a	b	A	A	B
%Chla	70.64 ± *6.60*	56.72 ± *2.45*	67.07	55.63 ± *3.77*	61.80 ± 3.51	67.07 ± 1.47	59.64 ± 2.34
	a	b	ab	b	A	A	B

Table 2. Mean values (±standard deviation) of zooplankton abundances from Zooscan and microscopic countings, percentage of taxonomic groups and total copepod demographic parameters at the stations for the four clusters defined in the PCA analysis on environmental variables (see Fig.2) and for the 3 long duration stations. W-MA = Western Melanesian archipelago, CE-MA= Central and Eastern Melanesian archipelago, BL = station B (blooming conditions) and GY = subtropical gyre. Letters below the mean values indicate homogeneous groups between zones (small letters) or LD stations (cap letters) according to post hoc Scheffé tests.

	W-MA	CE-MA	BL	GY	LD-A	LD-B	LD-C
Zooplankton Zooscan							
> 300 µm ESD (ind m^{-3})	718 ± 226	527 ± 120	678	250 ± 52	687 ± 233	678 ± 144	290 ± 72
	a	a	a	b	A	A	B
Zooplankton microscope							
Total (ind m^{-3})	1179 ± 370	1234 ± 358	1145	655 ± 213	1198 ± 520	1145 ± 175	784 ± 59
	ab	a	ab	b	A	A	B
> 300 µm ESD (ind m^{-3})	634 ± 169	724 ± 208	648	357 ± 91	684 ± 192	648 ± 103	404 ± 26
	ab	a	ab	b	A	A	B
% Copepods	73.1 ± 4.6	76.4 ± 3.1	77.4	82.3 ± 3.6	68.4 ± 11.6	77.4 ± 0.8	85.9 ± 1.9
	a	ab	ab	b	A	AB	B
% Gelatinous	18.6 ± 5.2	16.0 ± 3.1	14.7	11.9 ± 5.7	24.3 ± 11.4	14.7 ± 2.7	8.3 ± 1.6
	a	a	a	a	AB	A	B
% Other holoplankton	7.8 ± 3.5	6.7 ± 1.3	7.1	4.9 ± 2.4	6.4 ± 2.1	7.1 ± 2.2	5.3 ± 1.4
	a	a	a	a	A	A	A
% Meroplankton	0.6 ± 0.3	0.9 ± 0.6	0.8	0.9 ± 0.5	0.9 ± 0.2	0.8 ± 0.6	0.5 ± 0.2
	a	a	a	a	A	A	A
Copepods							
Total (ind m^{-3})	862 ± 17	943 ± 11	887	539 ± 8	834 ± 427	887 ± 144	659 ± 55
	a	a	a	b	A	A	A
% Nauplii	13.3 ± *3.1*	15.9 ± *9.6*	14.4	11.1 ± *7.1*	13.6 ± 5.5	14.4 ± 4.5	12.4 ± 4.3
	a	a	a	a	A	A	A
% Copepodites	68.3 ± 6.1	60.7 ± 10.7	67.0	74.3 ± 7.0	61.7 ± 2.8	67.0 ± 5.5	70.6 ± 4.7
	a	a	a	a	A	AB	B
% Adults	18.4 ± 6.8	23.3 ± 4.6	18.5	14.7 ± 2.2	24.7 ± 4.9	18.5 ± 2.7	17.0 ± 3.8
	a	a	a	a	A	AB	B
Sex ratio (% Females/Adults)	70.4 ± 8.3	79.7 ± 7.9	78.5	78.8 ± 5.9	62.6 ± 41.9	78.5 ± 7.9	78.9 ± 4.0
	a	a	a	a	A	A	A

Table 3: Mean values among stations of each cluster defined in the PCA analysis on environmental variables (±standard deviation) of zooplankton biomasses (top pannel) and percentage of total biomass for the different size fractions (bottom pannel) see Fig.2) and for the 3 long duration stations. Zooplankton biomasses estimated from weighting and from biovolume measurements from microscope and Zooscan observations. W-MA = Western Melanesian archipelago, CE-MA= Central and Eastern Melanesian archipelago, BL = station B (blooming conditions) and GY = subtropical gyre. Letters below the mean values indicate homogeneous groups between zones (small letters) or LD stations (cap letters) according to post hoc Scheffé tests.

	W-MA	CE-MA	BL	GY		LD-A	LD-B	LD-C
Biomass (mg DW m^{-3})								
Zooplankton (weighted)	12.2 ± 5.5 (a)	6.5 ± 4.0 (ab)	10.6 (ab)	2.5 ± 0.2 (b)		12.4 ± 2.1 (A)	10.6 ± 1.7 (A)	2.7 ± 0.4 (B)
Zooplankton(micro + zooscan)	5.7 ± 1.6 (a)	5.6 ± 1.9 (a)	8.9 (a)	2.0 ± 0.7 (b)		7.9 ± 2.9 (A)	8.9 ± 4.1 (A)	2.8 ± 1.3 (B)
Zooplankton <300 µm (micro)	0.3 ± 0.1 (a)	0.3 ± 0.1 (a)	0.3 (a)	0.2 ± 0.1 (a)		0.3 ± 0.2 (A)	0.3 ± 0.0 (A)	0.2 ± 0.0 (A)
Zooplankton >300 µm (Zooscan)	5.3 ± 1.4 (a)	5.2 ± 1.8 (ab)	8.6 (ab)	1.8 ± 0.7 (b)		7.6 ± 2.7 (A)	8.6 ± 4.1 (A)	2.6 ± 1.2 (B)
Detritus (Zooscan)	4.7 ± 1.6 (a)	2.9 ± 2.5 (ab)	3.9 (ab)	1.0 ± 0.0 (b)		7.0 ± 2.1	3.9 ± 1.2	1.0 ± 0.7
Zooplankton + Detritus	10.4 ± 3.1 (a)	8.5 ± 4.3 (a)	12.8 (ab)	3.0 ± 0.7 (b)		14.9 ± 2.6 (A)	12.8 ± 1.0 (A)	3.8 ± 1.0 (B)
%Detritus	44.9 ± 5.2 (a)	30.4 ± 10.9 (a)	30.7 (a)	35.2 ± 8.6 (a)		46.8 ± 13.4 (A)	30.7 ± 5.2 (AB)	26.5 ± 5.8 (C)
% Zooplankton biomass								
<300 µm (micro)	6.3 ± 3.5 (a)	6.0 ± 1.8 (a)	3.4 (a)	9.1 ± 2.8 (a)		4.0 ± 2.7 (A)	3.4 ± 1.1 (A)	8.3 ± 2.2 (B)
300-500 µm (Zooscan)	25.4 ± 5.1 (ab)	23.2 ± 3.0 (a)	17.4 (a)	33.1 ± 5.2 (b)		19.9 ± 5.1 (A)	17.4 ± 4.2 (A)	28.4 ± 7.9 (B)
500-1000 µm (Zooscan)	35.7 ± 6.4 (a)	33.1 ± 2.5 (ab)	33.0 (ab)	26.4 ± 0.9 (b)		32.3 ± 9.2 (A)	33.0 ± 4.9 (A)	27.2 ± 3.7 (A)
1000-2000 µm (Zooscan)	18.0 ± 7.0 (a)	21.1 ± 2.6 (a)	21.9 (a)	17.9 ± 3.8 (a)		23.5 ± 3.3 (A)	21.9 ± 4.1 (A)	20.3 ± 7.1 (A)
>2000 µm (Zooscan)	14.7 ± 7.2 (a)	16.6 ± 6.3 (a)	24.3 (a)	13.5 ± 4.7 (a)		20.4 ± 10.9 (A)	24.3 ± 10.0 (A)	15.9 ± 7.0 (A)

Table 4: Mean values (±standard deviation) per region of taxonomic diversity (H' = Shannon index) and taxonomic richness (nb taxa per sample) calculated for total zooplankton and copepod communities. W-MA = Western Melanesian archipelago, CE-MA= Central and Eastern Melanesian archipelago, BL = station B, blooming conditions, and GY = subtropical gyre. Letters below the mean values indicate homogeneous groups between zones (small letters) or LD stations (cap letters) according to post hoc Scheffé tests

	W-MA		CE-MA		BL	GY		LD-A		LD-B		LD-C	
H' zooplankton	3.54 ab	± 0.07	3.66 a	± 0.09	3.67 ab	3.40 b	± 0.10	3.50 A	± 0.04	3.67 B	± 0.11	3.40 C	± 0.04
nb taxa zooplankton	33.00 a	± 2.94	32.56 a	± 4.75	34.00 a	31.33 a	± 1.15	31.00 A	± 8.12	34.00 A	± 4.97	32.00 A	± 3.42
H' copepods	3.08 ab	± 0.08	3.14 a	± 0.09	3.13 ab	2.91 b	± 0.02	3.06 AB	± 0.18	3.13 A	± 0.08	2.92 B	± 0.06
nb taxa copepods	21.81 a	± 1.68	22.78 a	± 3.70	22.75 a	20.33 a	± 1.15	21.25 A	± 5.62	22.75 A	± 3.10	21.00 A	± 2.94

Table 5: Top 10 species in frequency abundance for the 4 regions (W-MA = Western Melanesian archipelago, CE-MA= Central and Eastern Melanesian archipelago, BL = station B, blooming conditions and GY = subtropical gyre).

Rank	W-MA	CE-MA	BL	GY
1	*Clauso/Paracalanus*	*Clauso/Paracalanus*	*Oncaea*	*Clauso/Paracalanus*
2	*Appendicularia*	*Oithona*	*Clauso/Paracalanus*	*Oithona*
3	*Oncaea*	*Oncaea*	*Oithona*	*Corycaeus*
4	*Oithona*	*Appendicularia*	*Appendicularia*	*Appendicularia*
5	*Nauplii*	*Nauplii*	*Nauplii*	*Oncaea*
6	*Corycaeus*	*Corycaeus*	*Microsetella*	*Nauplii*
7	*Thecosomata*	*Microsetella*	*Ostracoda*	*Microsetella*
8	*Microsetella*	*Thecosomata*	*Corycaeus*	*Thecosomata*
9	*Calocalanus*	*Ostracoda*	*Thecosomata*	*Calocalanus*
10	*Chaetognatha*	*Chaetognatha*	*Chaetognatha*	*Mecynocera clausi*

Table 6. Mean values (±standard deviation) of plankton stocks, zooplankton weight specific ingestion, respiration and excretion rates, zooplankton grazing, excretion and respiration fluxes, and zooplankton vertical fluxes. W-MA = Western Melanesian archipelago, CE-MA= Central and Eastern Melanesian archipelago, BL = station B, blooming conditions and GY = subtropical gyre. Letters below the mean values indicate homogeneous groups between zones (small letters) or LD stations (cap letters) according to post hoc Scheffé tests. Zooplankton stocks are estimated from cumulated biovolumes of binocular counted organisms. Swimmer biomasses in sediment trap from Caffin etal. (2018a).

	W - MA	CE - MA	BL	GY	LD-A	LD-B	LD-C
Plankton stocks							
Phytoplankton (mgC m^{-2})	1529 ± 268	1407 ± 291	2420	877 ± 92	1318 ± 147	2420 ± 458	819 ± 45
	a	a	a	b	A	A	B
POC (mgC m^{-2})	3974 ± 530	5165 ± 539	5957	3270 ± 569	4231	5957	2938
	a	b	b	a	A	A	B
Zooplankton (mgC m^{-2})	579 ± 256	682 ± 209	1038	227 ± 66	878 ± 331	1038 ± 193	290 ± 58
	a	ab	ab	b	A	A	B
weight specific rates							
Ingestion (d^{-1})	0.56 ± 0.01	0.50 ± 0.03	0.57	0.456 ± 0.01	0.57 ± 0.03	0.57 ± 0.02	0.45 ± 0.02
	a	bc	ab	c	A	A	B
NH$_4$ Excretion (d^{-1})	0.124 ± 0.012	0.115 ± 0.009	0.107	0.139 ± 0.021	0.122 ± 0.013	0.107 ± 0.008	0.115 ± 0.007
	a	a	a	a	A	A	A
PO$_4$ Excretion (d^{-1})	0.101 ± 0.009	0.096 ± 0.007	0.088	0.111 ± 0.014	0.100 ± 0.009	0.088 ± 0.006	0.095 ± 0.004
	a	a	a	a	A	A	A
Respiration (d^{-1})	0.239 ± 0.004	0.231 ± 0.003	0.245	0.224 ± 0.001	0.241 ± 0.003	0.245 ± 0.002	0.224 ± 0.001
	a	b	a	b	A	A	B
Grazing impact on phytoplankton							
Primary production (mgC m^{-2}d^{-1})	494 ± 128	352 ± 221	708	156 ± 26	663	708	173
	a	b	a	c			
ZCD$_H$ (mgC m^{-2} d^{-1})	169 ± 49	185 ± 60	426	82 ± 22	236 ± 120	426 ± 106	102 ± 24
	a	a	a	b	A	A	B
% Primary production	34.8 ± 7.6	72.6 ± 54.1	60.3	53.7 ± 16.6	35.7 ± 18.1	60.3 ± 15.0	58.9 ± 14.0
	a	b	ab	ab	A	A	A
% Phytoplankton stock d^{-1}							
% Total	11.5 ± 4.7	13.8 ± 5.8	17.6	9.4 ± 2.8	18.7 ± 10.9	18.9 ± 9.1	12.5 ± 3.2
	a	a	a	a	A	A	A
% Picoplancton	0.2 ± 0.1	0.3 ± 0.1	0.1	0.2 ± 0.0	0.3 ± 0.1	0.1 ± 0.0	0.2 ± 0.0
	a	a	a	a	A	A	A
% Nanoplankton	37.5 ± 10.8	43.6 ± 15.4	73.4	28.0 ± 52.9	8.9 ± 26.5	78.7 ± 38.2	37.7 ± 8.5
	a	a	b	a	A	B	A
% Microplankton	24.5 ± 18.6	30.0 ± 24.9	101.5	20.6 ± 19.3	52.9 ± 55.6	109.1 ± 53.2	42.8 ± 18.7
	a	a	b	a	A	B	A
NH$_4$ excretion impact on phytoplankton							
Phytoplankton needs (mgN m^{-2} d^{-1})	6.08 ± 1.69	3.32 ± 2.04	5.96	1.10 ± 0.34	8.28	5.96	1.46
	c	ab	bc	a			
Regeneration (mg N-NH$_4$ m^{-2} d^{-1})	1.75 ± 0.71	2.01 ± 0.66	2.75	0.77 ± 0.16	2.63 ± 0.94	2.75 ± 0.53	0.82 ± 0.13
	a	a	a	b	A	A	B
% N demand	29.7 ± 11.5	77.2 ± 43.8	46.2	75.4 ± 33.4	31.8 ± 11.3	46.2 ± 8.9	56.3 ± 10.8
	a	b	ab	b	A	AB	B
PO$_4$ excretion impact on phytoplankton							
Phytoplankton needs (mg P m^{-2} d^{-1})	0.38 ± 0.11	0.21 ± 0.13	0.37	0.07 ± 0.02	0.52	0.37	0.09
	a	bc	ab	c			
Regeneration (mg P-PO$_4$ m^{-2} d^{-1})	0.02 ± 0.01	0.03 ± 0.01	0.03	0.01 ± 0.00	0.03 ± 0.01	0.03 ± 0.01	0.01 ± 0.01
	a	a	a	b	A	A	B
% P demand	5.9 ± 2.3	15.6 ± 9.2	9.2	14.5 ± 6.2	6.3 ± 2.3	9.2 ± 1.7	11.2 ± 2.0
	a	b	ab	ab	A	AB	B
Zooplankton Respiration							
Respiration (mgC m^{-2} d$^{-1)}$)	137.2 ± 61.0	156.0 ± 47.3	248.8	50.6 ± 14.6	209.2 ± 79.2	248.8 ± 44.5	64.3 ± 12.2
	a	a	a	b	A	A	B
% Primary production	28.5 ± 12.1	59.9 ± 39.4	35.2	33.3 ± 11.0	31.6 ± 12.0	35.2 ± 6.3	37.1 ± 7.1
	a	a	a	a	A	A	A
Migratory Zooplankton below 200m							
Biomass (mg C m^{-2} d^{-1})					354.4 ± 80.1	189.7 ± 147.9	No migr.
Respiration (mg C m^{-2}d^{-1})					42.9 ± 16.2	25.3 ± 4.5	No migr.
Excretion N (mg N-NH$_4$ m^{-2} d^{-1})					0.55 ± 0.20	0.28 ± 0.05	No migr.
Excretion P (mg P-PO$_4$ m^{-2} d^{-1})					0.007 ± 0.002	0.003 ± 0.001	No migr.
Zooplankton in trap (150 m)							
Swimmer biomass (mg C m^{-2} d^{-1})					42.3 ± 7.6	57.1 ± 21.7	41.7 ± 14.8
					A	A	A

Table 7. Average zooplankton abundance and biomass values from different region of the western and central tropical South Pacific around the 20° parallel south.

Campain	Region	Lat.	Long.	Abundances (ind m^{-3})	Biomasses (mg DW m^{-3})	Reference
FLUPAC	Equator	0°	180°	-	14-18	Le Borgne et al (2003)
Hydrobios		8°S	180°	-	5	Le Borgne et al (1990)
BIOSOPE Bongot net, 200 µm	Marquisean islands	8.4°S	141°W	-	15-25	Carlotti (unpublished data)
OUTPACE Bongot net, 120µm	Coral Sea Feb-April 2015	17-22°S	160-170°E	800-1600	4-7.5	Present paper
19 oceanographic stations in New Caledonia.	Coral Sea	17-22°S	160-170°E	-	2-3	Le Borgne et al. (2011)
NECTALIS 1 HydrobiosMultiNet 200 µm	Coral Sea Cool seasonJuly 2011	17-22°S	160-170°E	200-400	2.5-6.9	Smeti et al (2015)
NECTALIS 2 HydrobiosMultiNet 200 µm	Coral Sea Hot season December 2011	17-22°S	160-170°E	150-250	2.0-2.8	Smeti et al (2015)
BIOSOPE Bongot net, 200 µm	SPSG	20°S	130-120°W	-	2-2.5	Carlotti (unpublished data)
OUTPACE Bongot net, 120 µm	GY	20°S	160-165°W	450-870	1.2-2.8	Present paper
PROCAL WP-2 net , 200 µm	Mahé	21,5°S	169°E	-	2.5-7	Le Borgne et al (1985)

Figures caption

Fig. 1.Transect of the OUTPACE cruise superimposed on quasi-Lagrangian weighted mean chl a of the WTSP during OUTPACE (see details in Moutin et al. 2017) with the two types of stations, short duration stations 1 to 15 (**x**) and long duration stations A, B and C (+). Along the transect, zooplankton samples were collected once at each short duration station, whereas day-night sampling were performed each day at three strategic long duration stations. Longitude is expressed as °E.

Fig. 2.PCA on environmental variables: Mixed-layer Depth (MLD); total Chl-*a* concentration (Chl-*a*+Phae), % Chl-*a*(ratio Chl-*a*/Chl-*a*+Phae), temperature, salinity averaged on the upper 0-200m of the water column. Plots of the 15 stations (A) and variables (B) on the first factorial plan. The green circles delimit the clusters defined at a distance of 3.3: W-MA = Western Melanesian archipelago, CE-MA= Central and Eastern Melanesian archipelago, BL = station B, blooming conditions and GY = subtropical gyre.

Fig. 3.Zooplankton abundances and biomasses along the OUTPACE West-East transect. (A) Abundances (ind m^{-3}) of small (ECD <300µm) and large (ECD >300µm) zooplankton determined by microscope counting (vertical bars), and of large zooplankton (ECD >300µm) determined by Zooscan (dark line). ==Averaged integrated== Chl-*a* concentrations (green line). (B) Cumulated zooplankton and detritus biomasses. Red line - values of total dry weight determined by weighting at each station. ==Black line total zooplankton biomass determined from microscopic counting==. Zooplankton biomass fraction < 300 µm was determined from microscopic counting. Zooplankton biomass fractions > 300 µm (4 fractions) and detritus biomass were estimated from Zooscanbiovolumes. SD-01 to 15: short duration stations. LD-A, LD-B and LD-C: long duration stations (average value and standard deviation over the 5 days sampling).

Fig 4. NDMS of the main zooplankton taxa (>0.1% abundance). A: Plot of the stations with different colors between the regions identified with the environmental clustering (4 regions: W-MA = Western Melanesian archipelago, CE-MA= Central and Eastern Melanesian archipelago, BL = Blooming conditions - station LD-B-; and GY = subtropical gyre). B: Plot of the taxa.

Fig 5. Spatial variation of (A) LOG10 transformed mean nifH abundance values for three groups of diazotrophs across the transect: *Trichodesmium*, HET-1 , UCYN-A and B grouped (Adapted from Stenegren et al., 2018, their Fig. 2b), abundance of (B)main copepod taxa and (C) main other zooplankton taxa.

Fig 6.Temporal variation of zooplankton abundance and biomass over 5 days at each of the three long duration stations (LD-A, LD-B and LD-C from left to right). (A)Abundances (ind m^{-3}) of small (ECD <300µm) and large (ECD >300µm)

zooplankton determined by microscope counting (vertical bars – only for days 1 and 5), and of large zooplankton (ECD >300µm) determined by Zooscan (dark line). Chl-*a* concentrations (green line). (B) Cumulated zooplankton biomass and detritus sampled. Red line - values of total dry weight determined by weighting at each station. The zooplankton biomass fraction < 300 µm was determined from microscopic counting. Zooplankton biomass fractions > 300 µm (4 fractions) and detritus biomass were estimated from Zooscan biovolumes.

Fig 7. Comparison of zooplankton abundance (orange trianles) and percentage of main taxa (bars) of zooplanktonic organisms (A) in the water column (0-200 m) and (B) in the sediment trap ("swimmers") at 150 m deep at each of the three long duration stations (LD-A, LD-B and LD-C from left to right. Sediment trap data at day 5 cannot be considered for the analysis (see Caffin et al, 2018a)

Fig. 8. A) Biomass weighted zooplankton and POM (5m depth) nitrogen isotope ratios (δ15N); B) Average percent contribution of diazotroph derived nitrogen (DDN) to zooplankton biomass (ZDDN). W-MA = Western Melanesian archipelago, CE-MA= Central and Eastern Melanesian archipelago, and GY = subtropical gyre.
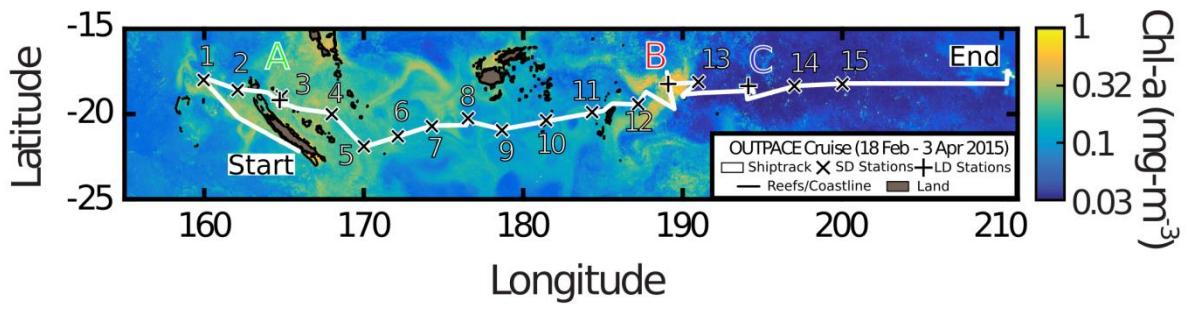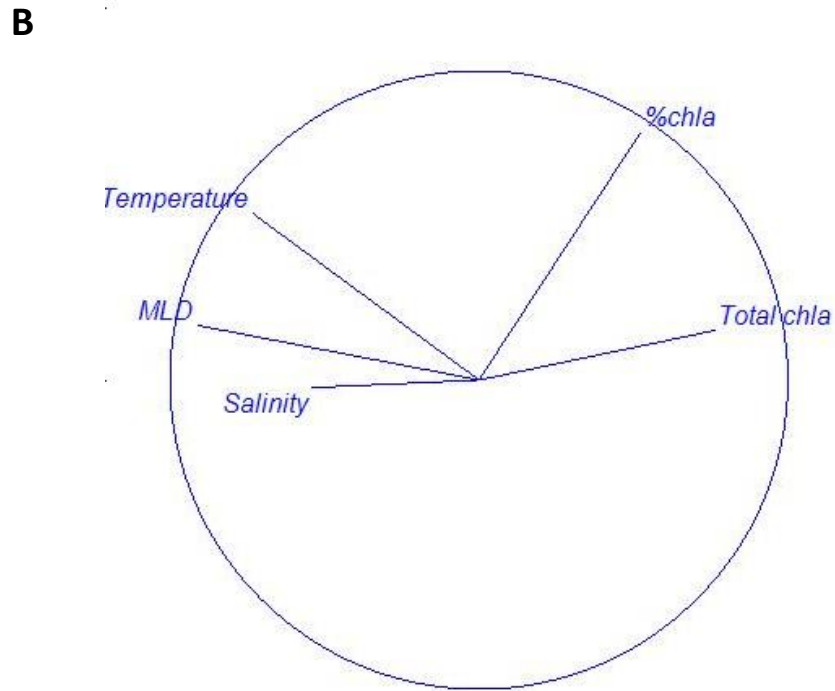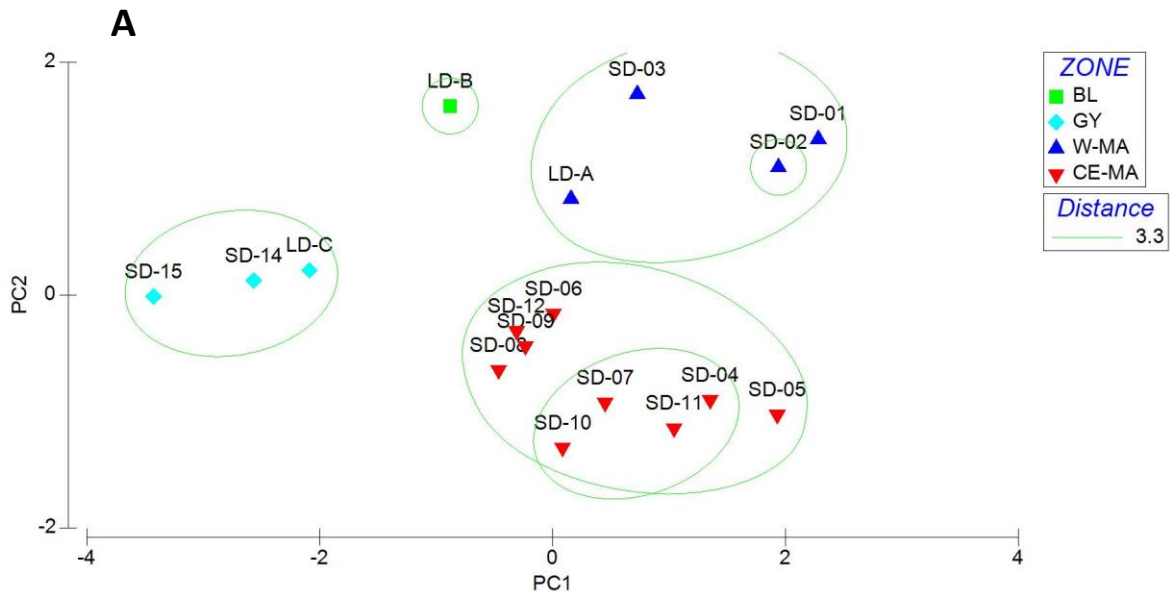
Figure 1

Figure 2.A,B
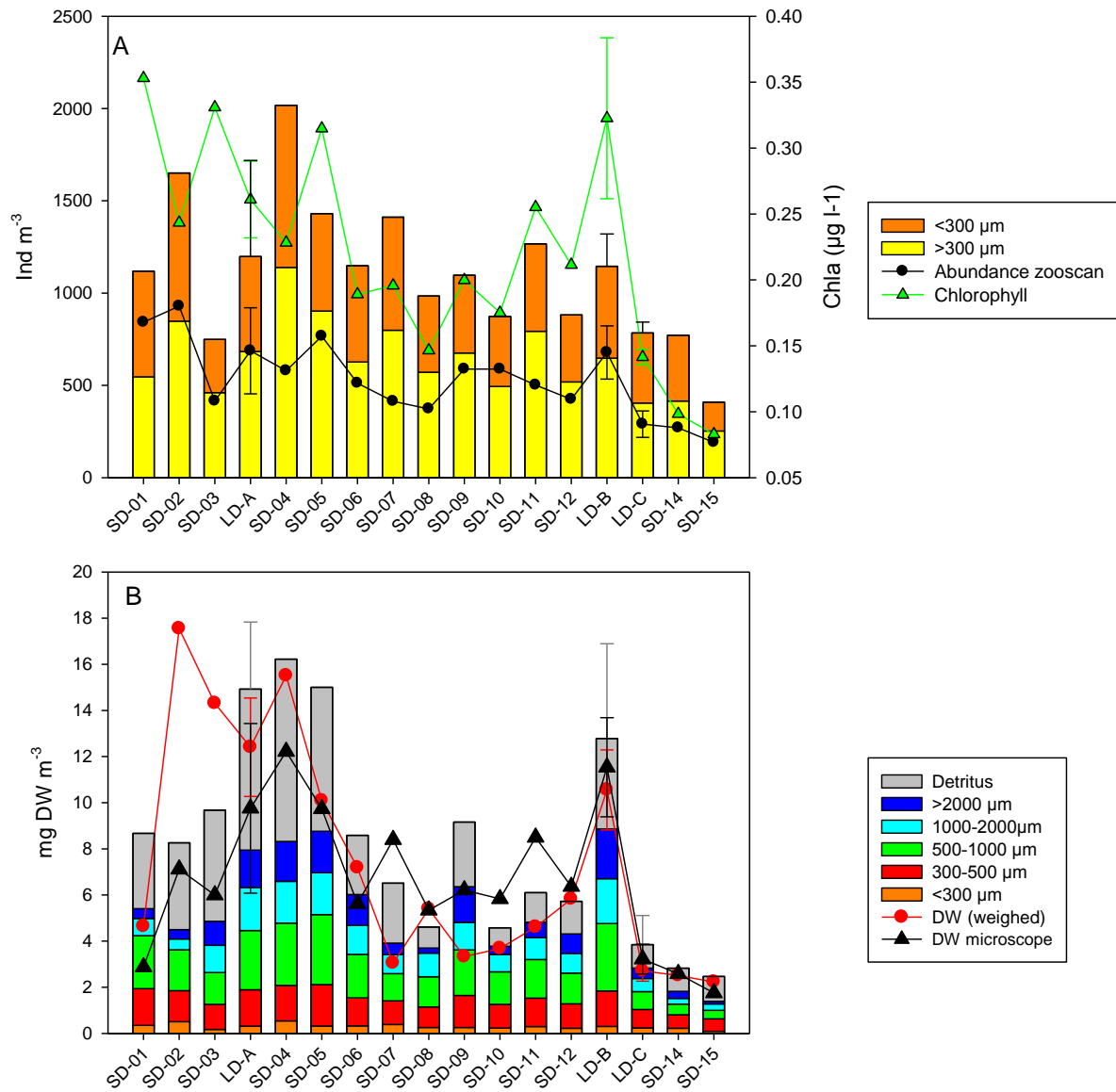
Figure 3.A,B

A
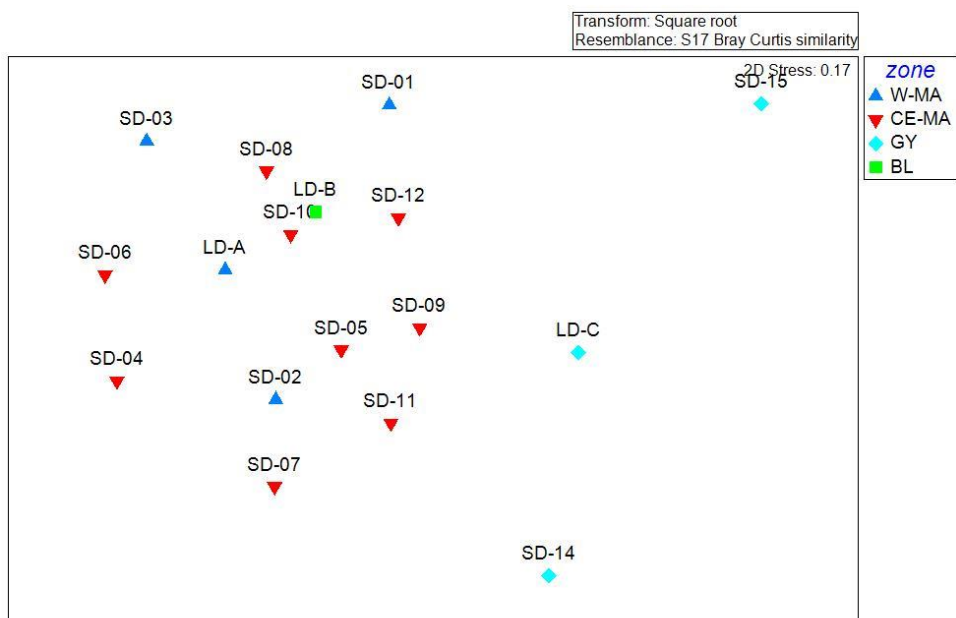
B
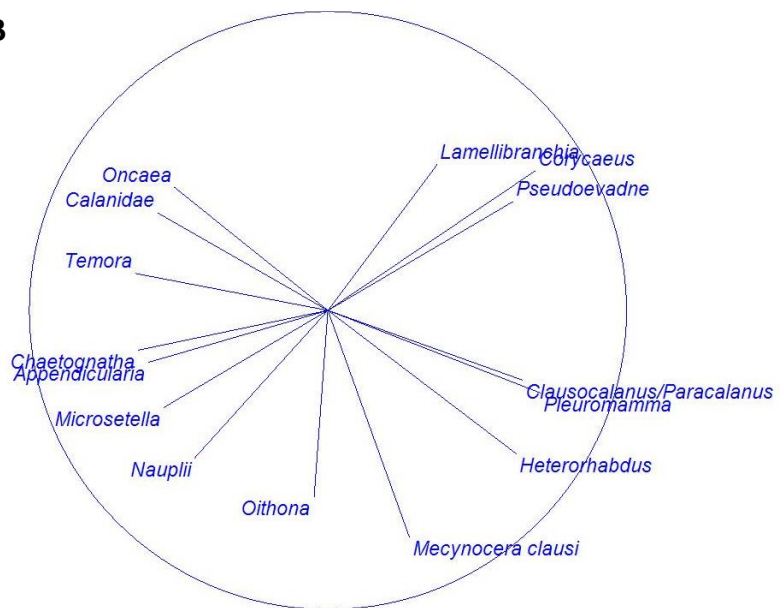
Figure 4A, B
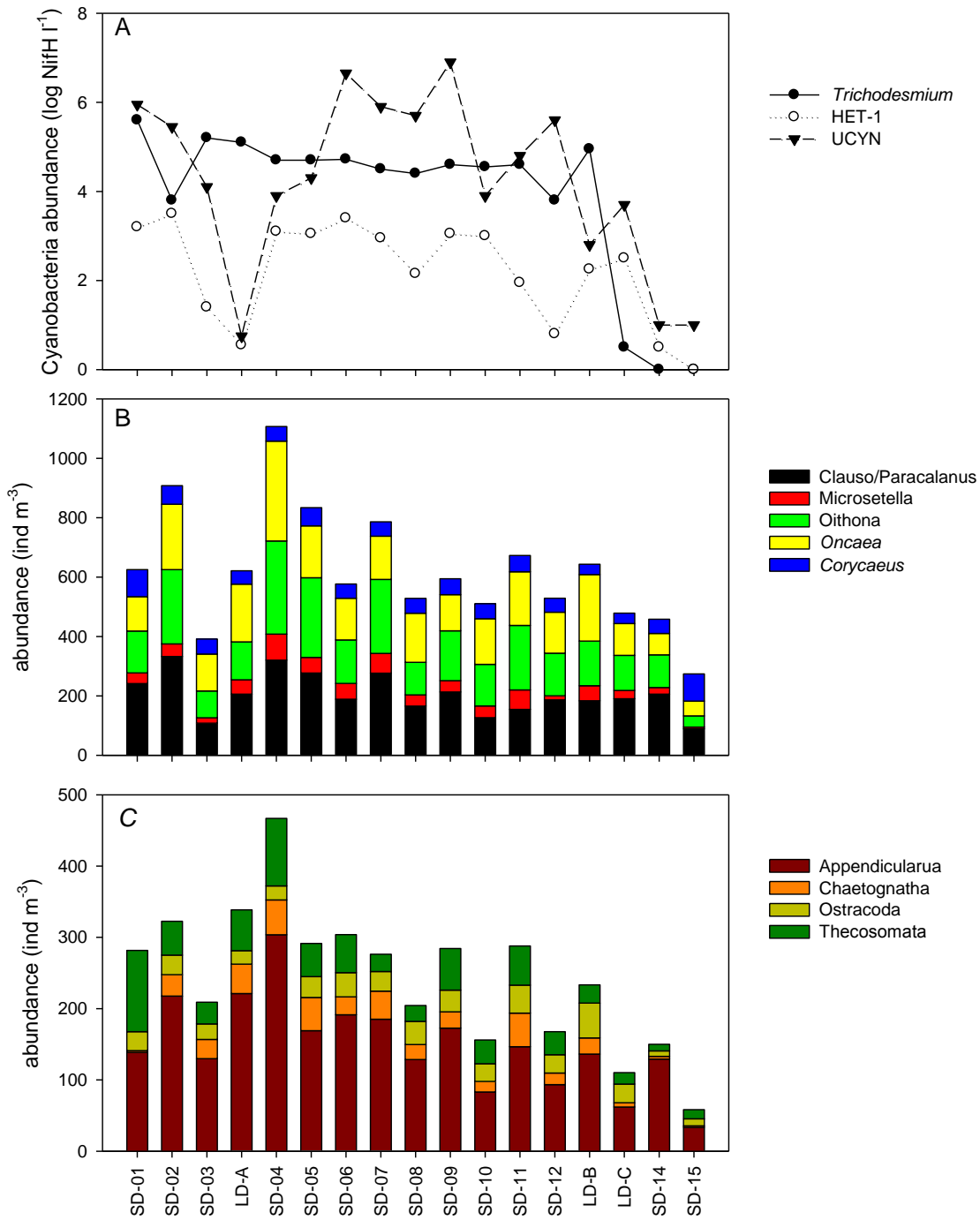
Figure 5 A, B,C
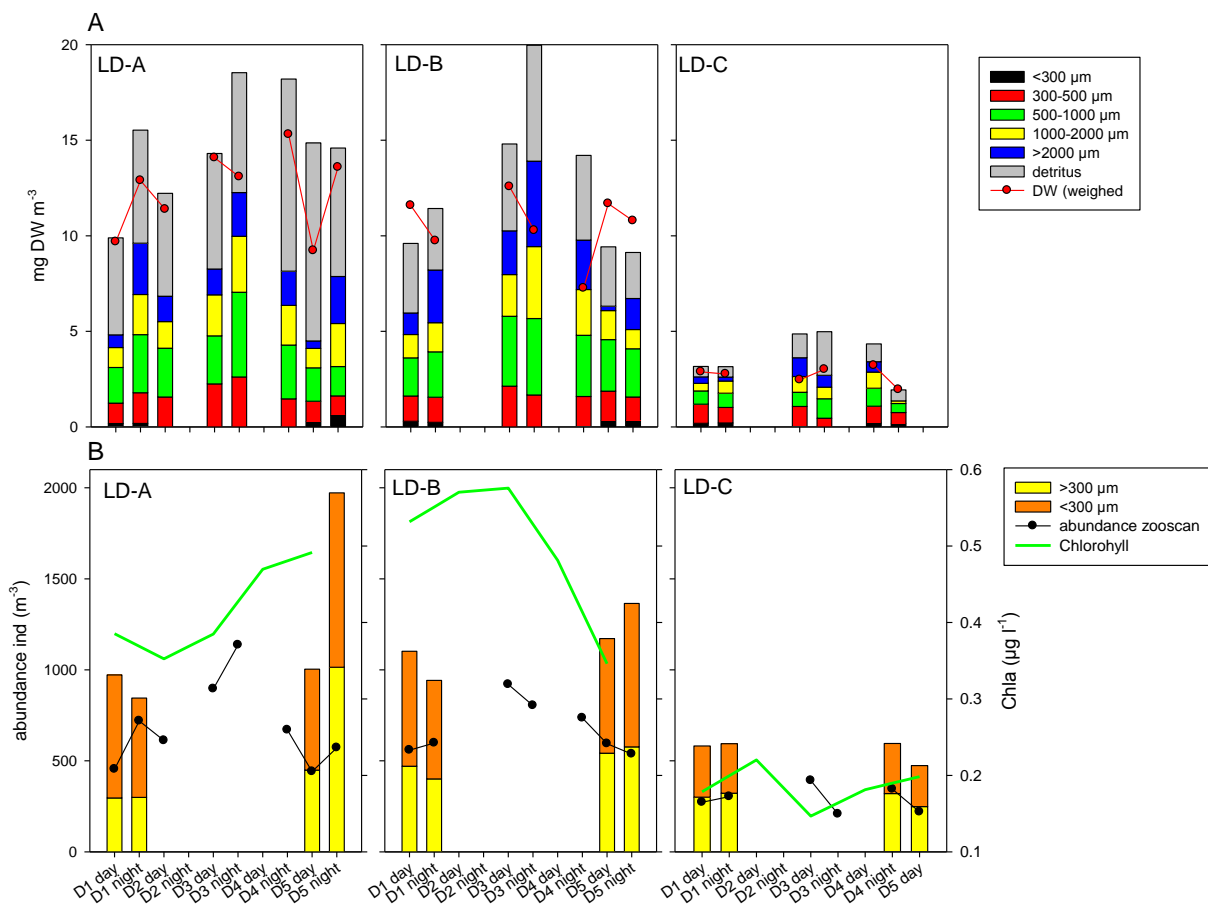
5   **Figure 6 A, B, C, D, E, F**
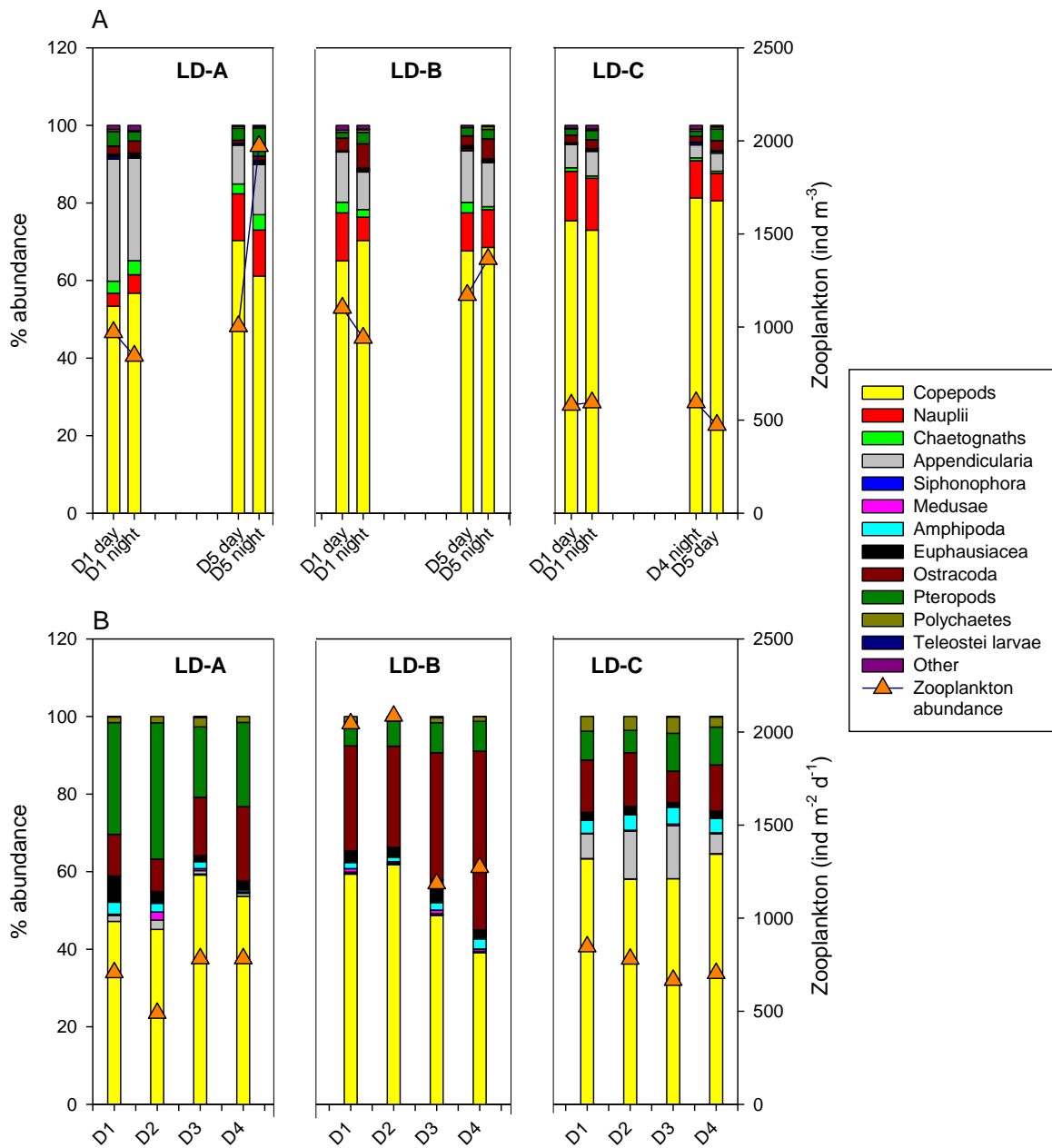
Figure 7 A, B
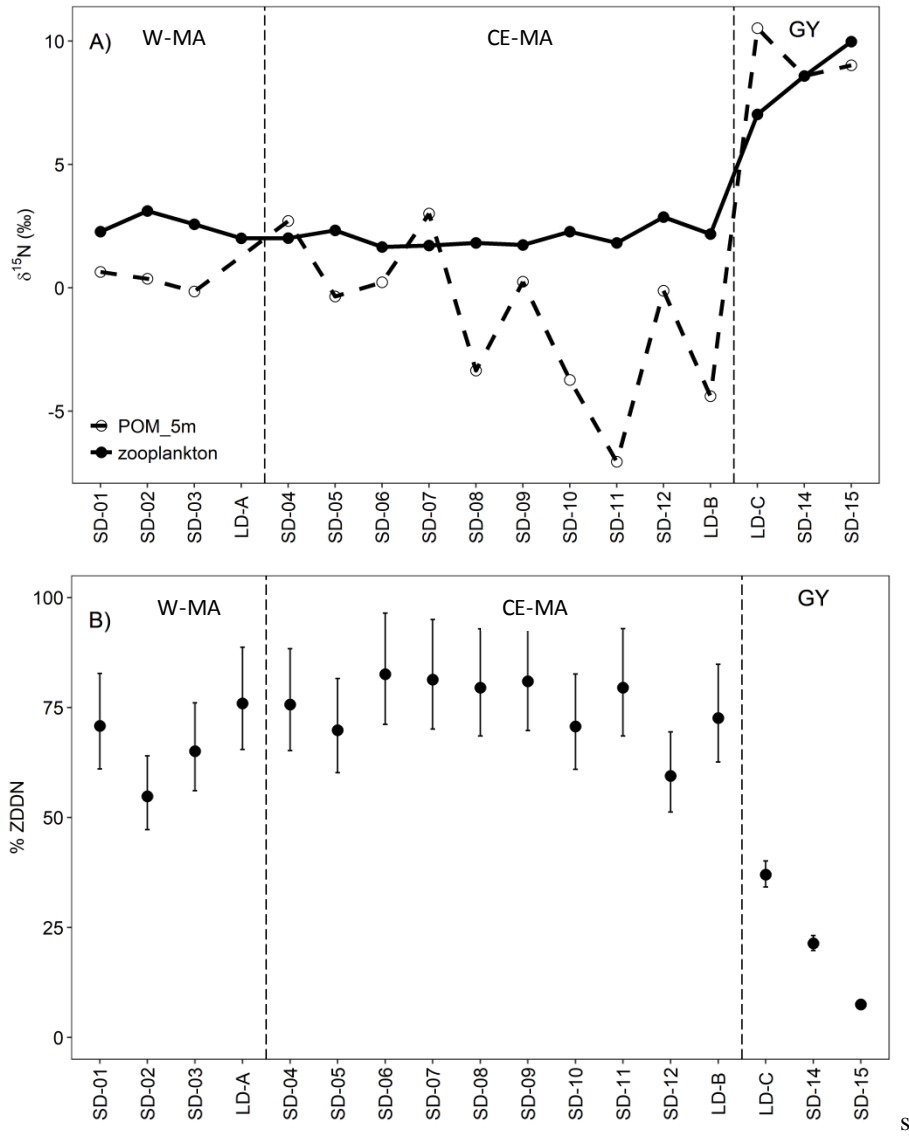
5   **Figure 8** A, B

Table S1 List of zooplanktonic taxa collected and identified during the 2015 OUTPACE cruise with average percentage of abundance within the 0-200 upper meters of the water column in the four Clusters defined in the PCA analysis on environmental variables. W-MA = Western Melanesian archipelago, CE-MA= Central and Eastern Melanesian archipelago, BL = station B, blooming conditions, and GY = subtropical gyre.

	W-MA	CE-MA	BL	GY		W-MA	CE-MA	BL	GY
COPEPODS					**COPEPODS (follow)**				
Copepod nauplii	10.02	8.96	9.63	9.22	*Phaenna spinifera*	0.01			
Undetermined copepodites	0.01				*Pleuromamma*	0.09	0.72	0.81	1.64
Acartia	0.76	0.95	0.12	0.65	*Sapphirina*	0.05	0.06	0.05	0.10
Aetideus		0.04			*Scaphocalanus*	0.01	0.03		
Calanidae	1.44	1.70	1.73	1.25	*Scolecithrix*	0.09	0.26		0.00
Calanopia	0.05	0.38	0.55	0.21	*Scottocalanus*		0.00		
Calanus	0.17	0.08	0.13	0.01	*Subeucalanus / Eucalanu*	0.09	0.01		
Calocalanus	2.68	1.81	1.34	1.53	*Temora*	0.60	0.34	0.33	0.07
Candacia	0.27	0.33	0.36	0.42	**OTHER CRUSTACEANS**				
Centropages	0.05	0.03		0.04	Amphipoda	0.02	0.01	0.15	0.04
Clausocalanus/Paracalanus	18.83	17.28	16.04	24.70	Euphausiacea	0.18	0.37	0.39	0.22
Clytemnestra	0.01	0.03	0.03		Lucifer	0.01	0.06		
Copilia	0.17	0.12	0.17	0.14	Ostracoda	2.01	2.38	4.26	2.22
Corycaeus	5.29	4.20	3.04	8.90	Pseudoevadne	0.04			0.34
Cosmocalanus darwini			0.05		**GELATINOUS**				
Ctenocalanus		0.12			Appendicularia	15.00	13.34	11.90	11.44
Cyclopoida		0.01		0.03	Doliole	0.18	0.09	0.39	0.21
Eucalanus	0.08	0.17	1.23	0.33	Salpidae	0.14	0.10	0.08	0.30
Euchaeta/Paraeuchaeta	0.06	0.10	0.03	0.07	Siphonophora	0.24	0.26	0.14	0.24
Euterpina acutifrons	0.02	0.06			Hydrozoa	0.06	0.06	0.19	0.04
Haloptilus	0.25	0.30	0.56	0.33	**CHAETOGNATHA**	2.13	2.56	1.98	0.60
Harpacticoida	0.01				**MOLLUSCS**				
Heterorhabdus	0.05	0.08	0.05	0.14	Thecosomata	5.29	3.81	2.24	1.95
Lubbockia	0.10	0.07	0.24	0.10	**MEROPLANKTON**				
Lucicutia	1.11	1.27	1.54	1.41	Decapod larvae	0.01	0.12		
Macrosetella gracilis	0.11	0.05	0.73	0.03	Cephalopod larvae	0.02			
Mecynocera clausi	1.20	1.64	1.17	2.03	Cirripedia larvae		0.01		
Mesocalanus/Neocalanus	0.08	0.05	0.18	0.07	Echinoderm larvae		0.02	0.03	
Microsetella	3.08	4.13	4.38	2.83	Lamellibranch larvae	0.17	0.41	0.12	0.32
Miracia efferata	0.01	0.05	0.08		Gasteropod larvae			0.08	
Mormonilla/Neomormonilla	0.08	0.23	0.13	0.12	Polychaets larvae	0.28	0.21	0.51	0.43
Nannocalanus minor	0.32	0.36	0.05	0.04	Teleostei eggs		0.06		
Oithona	12.90	15.89	13.16	13.54	Teleostei larvae		0.03	0.03	0.00
Oncaea	13.88	14.10	19.53	11.65	Branchiostoma	0.01			
Paracalanus	0.13	0.03	0.05	0.03	Larvae unknown	0.05	0.05	0.05	0.07